



This discussion paper is/has been under review for the journal Geoscientific Model Development (GMD). Please refer to the corresponding final paper in GMD if available.

Two soil hydrology formulations of ORCHIDEE (version Trunk.rev1311) tested for the Amazon basin

M. Guimbertea¹, P. Ciais^{1,2,3,4,5}, A. Ducharne^{1,2,6,7}, J. P. Boisier¹,
S. Peng^{1,2,3,4,5,8}, M. De Weirdt⁹, and H. Verbeeck⁹

¹Institut Pierre Simon Laplace (IPSL), France

²Centre National de la Recherche Scientifique (CNRS), Paris, France

³Laboratoire des Sciences du Climat et de l'Environnement (LSCE), 91191 Gif-sur-Yvette, France

⁴Joint Unit of Commissariat à l'énergie atomique et aux énergies alternatives (CEA), Gif-sur-Yvette, France

⁵Université de Versailles Saint-Quentin (UVSQ), Versailles, France

⁶Unité Mixte de Recherche (UMR) SISYPHE 7619, Paris, France

⁷Université Pierre et Marie Curie (UPMC), Paris, France

⁸UJF Grenoble 1, Laboratoire de Glaciologie et Géophysique de l'Environnement (LGGE, UMR5183), Grenoble, France

⁹Laboratory of Plant Ecology, Department of Applied Ecology and Environmental Biology, Faculty of Bioscience Engineering, Ghent University, Coupure Links 653, 9000 Ghent, Belgium

GMDD

7, 73–129, 2014

Two soil hydrology
formulations tested
for the Amazon basin

M. Guimbertea et al.

Title Page

Abstract

Introduction

Conclusions

References

Tables

Figures



◀

▶

Back

Close

Full Screen / Esc

Printer-friendly Version

Interactive Discussion



Received: 21 November 2013 – Accepted: 17 December 2013 – Published: 7 January 2014

Correspondence to: M. Guimberteau (matthieu.guimberteau@upmc.fr)

Published by Copernicus Publications on behalf of the European Geosciences Union.

GMDD

7, 73–129, 2014

**Two soil hydrology
formulations tested
for the Amazon basin**

M. Guimberteau et al.

[Title Page](#)

[Abstract](#)

[Introduction](#)

[Conclusions](#)

[References](#)

[Tables](#)

[Figures](#)



[Back](#)

[Close](#)

[Full Screen / Esc](#)

[Printer-friendly Version](#)

[Interactive Discussion](#)



Abstract

This study analyzes the impact of the two soil model parameterizations of the Land Surface Model ORCHIDEE on their estimates of Amazonian hydrology and phenology for five major sub-basins (Xingu, Tapajós, Madeira, Solimões and Negro), during the 29 yr

period 1980–2008. The two soil models are a simple 2 layer soil scheme with a bucket topped by an evaporative layer vs. an 11 layer soil diffusion scheme. The soil models were coupled with a river routing module and a process model of plant physiology, phenology and carbon dynamics. The simulated water budget and vegetation functioning components were compared with several datasets at sub-basin scale. The use of the 11 layer soil diffusion scheme did not significantly change the Amazonian water budget simulation when compared to the 2 layer soil scheme (+3.1 and –3.0 % in evapotranspiration and river discharge, respectively). However, the higher water holding capacity of the soil and the physically based representation of runoff and drainage in the 11 layer soil diffusion, resulted in higher dynamics of soil water storage variation and improved simulation of the total terrestrial water storage when compared to GRACE satellite estimates. The greater soil water storage within the 11 layer soil diffusion scheme resulted in increased dry-season evapotranspiration ($+0.5 \text{ mm d}^{-1}$, +17 %) and river discharge in the southeastern sub-basins such as the Xingu. Evapotranspiration over this sub-basin was sustained during the whole dry season with the 11 layer soil diffusion model, whereas the 2 layer soil scheme limited it at the end of the dry season. Lower plant water stress simulated by the 11 layer soil diffusion scheme, led to better simulation of the seasonal cycle of photosynthesis (GPP) when compared to a GPP data-driven model based upon eddy-covariance and satellite greenness measurements. Simulated LAI was consequently higher with the 11LAY (up to +0.4) but exhibited too low a variation when compared to a satellite-based dataset. The dry-season length between 4 and 7 months over the entire Amazon basin was found to be critical in distinguishing differences in hydrological feedbacks between the soil and the vegetation cover simulated by the two soil models. Overall, the 11 layer soil diffusion scheme provided little

Two soil hydrology formulations tested for the Amazon basin

M. Guimberteau et al.

[Title Page](#)

[Abstract](#)

[Introduction](#)

[Conclusions](#)

[References](#)

[Tables](#)

[Figures](#)

◀

▶

◀

▶

[Back](#)

[Close](#)

[Full Screen / Esc](#)

[Printer-friendly Version](#)

[Interactive Discussion](#)



[Title Page](#)[Abstract](#)[Introduction](#)[Conclusions](#)[References](#)[Tables](#)[Figures](#)[◀](#)[▶](#)[◀](#)[▶](#)[Back](#)[Close](#)[Full Screen / Esc](#)[Printer-friendly Version](#)[Interactive Discussion](#)

improvement in simulated hydrology on average over the wet tropical Amazonian sub-basins but a more significant improvement over the drier sub-basins. However, the use of the 11 layer soil diffusion scheme might become critical for assessments of future hydrological changes, especially in southern regions of the Amazon basin where longer dry season and more severe droughts are expected in the next century.

1 Introduction

Not only is the hydrological functioning of the Amazon basin complex but the river also makes a large contribution to the volume of fresh water discharged into the oceans (15–20 % of the total volume, Molinier and Guyot, 1996). The Amazon basin has therefore been the subject of many hydrological modeling studies (Coe et al., 2007; Decharme et al., 2008; Beighley et al., 2009; Trigg et al., 2009; Fan and Miguez-Macho, 2010; Geitirana et al., 2010; Paiva et al., 2011, 2012; Yamazaki et al., 2011, 2012; Guimbarteau et al., 2012a; Miguez-Macho and Fan, 2012a, b). The large area of the basin (about 6 million km²) encompasses a large range of precipitation (P) and river discharge (Q), the seasonality of which is further modulated by floodplains.

The total terrestrial water storage (TWS) (Ramillien et al., 2008) plays an important role in regulating the global climate (Famiglietti, 2004). TWS can be estimated by measuring the average amount of water in a basin. The Gravity Recovery And Climate Experiment (GRACE) satellite mission provided the first global observations of TWS, based on variation in the Earth's gravity field. TWS is directly comparable to model outputs for water balance assessment over large river basins (Schmidt et al., 2006, 2008; Syed et al., 2008; Jin and Feng, 2013). Some Land Surface Models (LSMs) have included river routing schemes that account for water storage in the river system to simulate the delay between precipitation over the basin and runoff at the river's mouth (Polcher, 2003; Alkama et al., 2010). Such schemes give better predictions of TWS (Ngo-Duc et al., 2007). GRACE observations over the Amazon basin improved the characterization of the spatio-temporal variability of the amount of water in the Amazon

Two soil hydrology formulations tested for the Amazon basin

M. Guimbetteau et al.

[Title Page](#)

[Abstract](#)

[Introduction](#)

[Conclusions](#)

[References](#)

[Tables](#)

[Figures](#)

◀

▶

[Back](#)

[Close](#)

[Full Screen / Esc](#)

[Printer-friendly Version](#)

[Interactive Discussion](#)



basin (Xavier et al., 2010; Becker et al., 2011), led to the identification of the factors responsible for differences between modeled discharge and observed river flow (Syed et al., 2005) and to the evaluation of the different contributions of the components of the annual water mass balance (Crowley et al., 2008; Frappart et al., 2013). Regional studies also investigated water storage over Amazonian sub-basins such as the Rio Negro tributary (Frappart et al., 2008, 2011). Moreover, the GRACE TWS products have also proven to be reliable for assessment of extreme events, such as Amazonian floods (Chen et al., 2010) and droughts (Chen et al., 2009; Frappart et al., 2012).

Soil moisture change makes an important contribution to change in TWS. In turn, soil moisture variations influence the partitioning of net radiation into sensible vs. latent heat flux at the surface, and consequently the ratio of turbulent fluxes through the atmospheric boundary layer. The role of soil moisture in controlling evapotranspiration (ET) is important over the Amazon basin, and particularly in south Amazonia, where a high rate of water recycling is sustained (Marengo, 2006) through transpiration (Shuttleworth, 1988). Thus, soil moisture parametrization in LSMs plays a critical role in accurate modeling of the hydro-climatology and CO₂ fluxes. In addition, accurate soil moisture modeling is needed to represent the feedbacks between the land surface and the atmosphere, which are one of the main sources of uncertainty in climate models (Douville, 2010; Koster et al., 2004b). Multilayer schemes have been introduced in LSMs to better describe the water diffusion through the soil (Thompson and Pollard, 1995; Viterbo and Beljaars, 1995; Chen et al., 1997; Cox et al., 1999; Boone et al., 2000; De Rosnay et al., 2000; Dai et al., 2003; Decharme et al., 2011). These schemes have improved ET modeling compared to simpler representations of the soil, as shown by the results of global scale simulations and comparison with local measurements (De Rosnay et al., 2002). Moreover, the physical characteristics of the soil taken into account in these multilayer schemes result in better representation of the impact of soil hydrology on land–atmosphere exchanges (Guillod et al., 2013).

The main question we address in this study is “Does the use of an 11 layer soil diffusion scheme, rather than a simpler 2 layer scheme, improve the simulation of water

Two soil hydrology formulations tested for the Amazon basin

M. Guimbarteau et al.

[Title Page](#)

[Abstract](#)

[Introduction](#)

[Conclusions](#)

[References](#)

[Tables](#)

[Figures](#)

◀

▶

◀

▶

[Back](#)

[Close](#)

[Full Screen / Esc](#)

[Printer-friendly Version](#)

[Interactive Discussion](#)



2 Model description

2.1 General Land Surface Model

ORCHIDEE is an LSM simulating energy, water fluxes, CO₂ and ecosystem carbon cycling. It is the land component of the Institut Pierre Simon Laplace (IPSL) coupled climate model. In uncoupled simulations, feedbacks with the atmosphere are removed and the model is run offline, a mode frequently used to test model performance when compared to observations, as in this study. ORCHIDEE includes two main modules:

1. The Surface–Vegetation–Atmosphere Transfer scheme (SVAT) SECHIBA (Schématisation des Echanges Hydriques à l'Interface entre la Biosphère et l'Atmosphère, Ducoudré et al., 1993; De Rosnay and Polcher, 1998) simulates energy and water exchanges between the atmosphere and the land surface, and the resulting soil water budget. SECHIBA includes two possible configurations to represent soil hydrological processes (Sect. 2.2) whose results are evaluated in this study.
2. Phenology and carbon dynamics are simulated by the STOMATE (Saclay Toulouse Orsay Model for the Analysis of Terrestrial Ecosystems, Viovy, 1996) module (Sect. 2.3) coupled with SECHIBA. STOMATE links the fast hydrological and biophysical processes of SECHIBA with the carbon dynamics (photosynthesis, allocation, biomass change and mortality, litter and soil carbon decomposition). Further, STOMATE calculates plant phenology, driven by climatic and biotic factors such as leaf age. The Dynamic Global Vegetation Model (DGVM) LPJ (Lund-Postdam-Jena, Sitch et al., 2003) includes all the parameterizations of the vegetation dynamics such as tree mortality, fire, etc. For this study, this module has not been activated.

Title Page

Abstract

Introduction

Conclusions

References

Tables

Figures

◀

▶

Back

Close

Full Screen / Esc

Printer-friendly Version

Interactive Discussion



2.2 Soil hydrology modeling with SECHIBA

- SECHIBA is the physical module of ORCHIDEE and simulates water and energy fluxes between the soil and the atmosphere through the vegetation, at a 30 min time step. Two soil hydrological schemes (the 2 layer soil scheme and the 11 layer soil diffusion scheme) are available to simulate the soil water fluxes and storage, controlling runoff and ET fluxes. In both models, ET is the sum of evaporation of water intercepted by the canopy, transpiration of vegetation which is related to water availability in the soil and to a fixed root density profile (De Rosnay and Polcher, 1998), bare soil evaporation related to water availability in the soil, snow sublimation and floodplains evaporation.
- We give here a brief description of the two soil models. These models have the same 2 m soil depth and are both coupled to STOMATE and the same routing model. More details are given by Ducoudré et al. (1993) and Guimbarteau et al. (2012b) for the 2 layer soil scheme, and by De Rosnay et al. (2000, 2002), D'Orgeval et al. (2008) and Campoy et al. (2013) for the 11 layer soil diffusion scheme.

2.2.1 2 layer soil scheme

The 2 layer soil scheme (Ducoudré et al., 1993) (hereafter called "2LAY") is frequently used with the STOMATE module, and recently for the Coupled Model Intercomparison Project Phase 5 (CMIP5) IPCC (Intergovernmental Panel on Climate Change) climate scenarios. It is an idealized model in which field capacity is set to 300 kg m^{-2} over a two-meter soil depth. The hydrological scheme is represented by two layers linked by a drainage flux (Ducharne et al., 1998). The top layer is subject to bare soil evaporation limited by a resistance (Ducoudré et al., 1993) and root extraction. The amount of water stored in this layer is directly controlled by rain falling through the canopy and the top layer can disappear when its water content is fully evaporated. The water content in the deep layer depends only to water extraction by the root profile. Runoff is computed as in the bucket model of Manabe (1969) and occurs only when the soil bucket is saturated. The total soil water excess gives runoff, which can be considered as Dunne

GMDD

7, 73–129, 2014

Two soil hydrology formulations tested for the Amazon basin

M. Guimbarteau et al.

Title Page	
Abstract	Introduction
Conclusions	References
Tables	Figures
◀	▶
◀	▶
Back	Close
Full Screen / Esc	
Printer-friendly Version	
Interactive Discussion	



runoff (Dunne and Black, 1970). This flux is assumed to be partitioned into 95 % deep drainage and 5 % surface runoff. The water budget is computed separately for each Plant Functional Type (PFT) tile within the mesh and then averaged over the grid cell. In the 2LAY, soil texture does not influence field capacity.

5 2.2.2 11 layer soil diffusion scheme

The second hydrological model is the 11 layer soil diffusion scheme (De Rosnay et al., 2000, 2002; D'Orgeval, 2006; Campoy et al., 2013), hereafter called "11LAY". It has been used for streamflow evaluation (Guimbarteau et al., 2012a) and for studying future annual extreme flow variation under climate change, for the Amazon basin (Guimbarteau et al., 2013). The 11LAY scheme simulates vertical soil flow based on physical processes from the Fokker–Planck equation that resolves water diffusion in non-saturated conditions from the Richards equation (Richards, 1931). The 2 m soil column is divided into 11 discrete layers whose thickness increases geometrically downward with depth. Soil texture heterogeneity between grid cells is taken into account by employing three different soil types (coarse, medium and fine textured). Their spatial distribution is diagnosed by interpolating the Food and Agriculture Organization texture map (FAO, 1978) by Zobler (1986) at a scale of $1^\circ \times 1^\circ$, considering only the dominant soil type on each grid cell. In ORCHIDEE, the five textural classes (coarse, medium-coarse, medium, medium-fine and fine) are reduced to three, with ORCHIDEE's medium class grouping the Zobler classes of medium-coarse, medium and medium-fine. At the working ORCHIDEE resolution, only the dominant texture in each grid cell is used. The relationships between hydraulic conductivity, volumetric water content and matrix potential are described in ORCHIDEE by the Mualem–Van Genuchten model (Mualem, 1976; Van Genuchten, 1980), using parameters estimated by Carsel and Parrish (1988) for the corresponding soil texture classes of the United States Department of Agriculture (USDA). The maximal soil water content in the 2 m soil is between 820 kg m^{-2} (coarse and fine classes) and 860 kg m^{-2} (medium class) depending on soil texture. The saturated hydraulic conductivity is modified (D'Orgeval et al., 2008) to take into account

[Title Page](#)[Abstract](#)[Introduction](#)[Conclusions](#)[References](#)[Tables](#)[Figures](#)[◀](#)[▶](#)[Back](#)[Close](#)[Full Screen / Esc](#)[Printer-friendly Version](#)[Interactive Discussion](#)

two properties that have opposite effects on conductivity (Beven and Germann, 1982; Beven, 1984): (1) increased soil compactness with depth and (2) enhanced infiltration capacity due to the presence of vegetation that increases soil porosity in the root-zone. The vertically explicit modeling of soil water fluxes enables a more physically-based runoff computation than is achieved in 2LAY (De Rosnay et al., 2002). The precipitation rate and capacity of the soil to infiltrate govern the production of runoff that can be assigned to Hortonian runoff (Horton, 1933). The precipitation partitioning between surface runoff and soil infiltration is parameterized through a time-splitting procedure according to Green and Ampt (1911) where the wetting front moves with time through the soil layers (D'Orgeval et al., 2008). Free gravitational drainage occurs at the bottom of the soil (bottom boundary condition). Independent water budgets are computed over three groups of PFTs (grouping bare soil, trees, and grass/crops) within each grid cell and then averaged over the grid cell.

2.3 Vegetation modeling with STOMATE

- In each grid cell, up to twelve PFTs can be represented simultaneously, in addition to bare soil. In the Amazon basin, the dominant PFT is “Tropical broad-leaved evergreen forest” (83 %) compared to “C4 grassland” (7 %), “C3 grassland” (5 %), “Tropical broad-leaved rainforest” (3 %) and others (2 %). Their fraction is adapted from the 1 km global land cover map (International Geosphere Biosphere Programme (IGBP), Belward et al., 1999) reduced by a dominant-type method to 5 km spatial resolution with the Olson classification (Olson et al., 1983). Maximal fraction of vegetation is thus defined for each grid cell. It is modulated by the Leaf Area Index (LAI) growth, specific to each PFT represented in the model. LAI dynamics (from carbohydrate allocation) is simulated by STOMATE which deals with the allocation of assimilates, autotrophic respiration components, foliar development, mortality and soil organic matter decomposition. The water stress of the vegetation influences only the photosynthetic capacity. A factor of representing water stress (McMurtrie et al., 1990) linearly computes the rate of Ribulose Biphosphate (RuBP) regeneration and the carboxylation rate.



2.4 River routing module

The routing module (Polcher, 2003; Guimbarteau et al., 2012a) calculates the daily continental runoff to the ocean. This scheme is based on a parametrization of water flows on a global scale (Miller et al., 1994; Hagemann and Dumenil, 1998). The global map of the major watersheds (Oki et al., 1999; Fekete et al., 1999; Vörösmarty et al., 2000) delineates the basin boundaries and allocates one of eight possible directions to the water flow within each grid cell. The $0.5^\circ \times 0.5^\circ$ resolution of the basin map is higher than the atmospheric forcing resolutions commonly used and it is therefore possible to have more than one basin in an ORCHIDEE grid cell (sub-basins). Water between each sub-grid basin is transferred through three linear water reservoirs, with no direct interaction with the atmosphere (except over floodplain areas). In each sub-basin, surface runoff and deep drainage are transformed into river discharge corresponding to fast and slow reservoirs, respectively. Both discharges feed the stream reservoir of the next downstream sub-basin, which also receives the discharge from all upstream sub-basins. Travel time within the reservoirs depends on their different residence times. The residence time is the product of a water retention index and a velocity constant. For each grid cell, the water retention index is given by a $0.5^\circ \times 0.5^\circ$ resolution map obtained by a simplification of Manning's formula (Manning, 1895; Ducharme et al., 2003). This retention index is common to all three reservoirs in a grid cell but varies between grid cells, depending on topography. The velocity constant does not vary spatially but distinguishes the three reservoirs. The corresponding three values of the velocity constant have been calibrated over the Senegal basin with the 2LAY parameterization (Ngo-Duc et al., 2007) and generalized for all the basins of the world. The stream reservoir has the highest velocity constant (4.2 m d^{-1}), which is lower in the fast reservoir (0.33 m d^{-1}) and still lower in the slow reservoir (0.04 m d^{-1}). However, when the 11LAY parameterization was used, the velocity constant of the slow reservoir was increased to the one of the fast reservoir (D'Orgeval, 2006). The goal was to simulate consistent river discharge between both soil models despite a higher residence time of water in the soil

Two soil hydrology formulations tested for the Amazon basin

M. Guimbarteau et al.

[Title Page](#)

[Abstract](#)

[Introduction](#)

[Conclusions](#)

[References](#)

[Tables](#)

[Figures](#)

◀

▶

[Back](#)

[Close](#)

[Full Screen / Esc](#)

[Printer-friendly Version](#)

[Interactive Discussion](#)



when using 11LAY parameterization. However, in order to facilitate the detection of the effect of the soil model parameterization on the TWS, we changed the velocity constant of the slow reservoir for the 11LAY model and set it equal to the one used in the 2LAY.

The routing scheme also includes a floodplain/swamp parameterization (D'Orgeval et al., 2008), recently improved by Guimberteau et al. (2012a) for the Amazon basin, by means of a new floodplain map. Over the floodplain areas, the water from the upstream reservoirs is delayed in a floodplain reservoir before going into the stream reservoir. The velocity constant of the floodplain reservoir, for both soil hydrology models, is the same (0.4 m d^{-1}) and equal to that found by Guimberteau et al. (2012a) who calibrated it for the Amazon basin.

3 Methods and dataset

3.1 Simulation design and forcing datasets

ORCHIDEE is forced by the Princeton Global Forcing (Sheffield et al., 2006) at a $1^\circ \times 1^\circ$ spatial resolution. It is based on the National Center for Environmental Prediction–National Center for Atmospheric Research (NCEP–NCAR) reanalysis datasets (Kistler et al., 2001). The temporal resolution is three hours and the time series cover the period 1948–2008. All the required forcing variables (Table 1) come directly from NCEP–NCAR, except the precipitation. The latter has been corrected using the monthly CRU (Climatic Research Unit) dataset (New et al., 2000) and statistically downscaled from $2^\circ \times 2^\circ$ to $1^\circ \times 1^\circ$ resolution using relationships developed with the Global Precipitation Climatology Project (GPCP, Huffman et al., 2001) daily product. A similar method has been used to disaggregate from daily to three hourly using the Tropical Rainfall Measuring Mission (TRMM, Huffman et al., 2007) satellite data product. For this study, the precipitation data were further corrected by the new product (Version 5) of GPCC (Global Precipitation Climatology Centre, Schneider et al., 2013) (1901–2009), which

[Title Page](#)[Abstract](#)[Introduction](#)[Conclusions](#)[References](#)[Tables](#)[Figures](#)[◀](#)[▶](#)[Back](#)[Close](#)[Full Screen / Esc](#)[Printer-friendly Version](#)[Interactive Discussion](#)

seems to be the better global product for hydrological applications (Decharme and Douville, 2006).

Two simulations with the 2LAY and the 11LAY were performed using SECHIBA coupled with STOMATE, the routing scheme and the floodplain parameterization. Each simulation was conducted for 34 yr (1975–2008), the first 5 yr of the period being discarded in order to ensure a state of hydrological equilibrium at the beginning of the analyzed time series. Thus, the 29 yr period from 1980–2008 was analyzed for the Amazon basin and its five large sub-basins: the Madeira, Tapajós and Xingu in the south, the Solimões in the west and the Negro in the north (Fig. 1).

10 3.2 Evaluation datasets

Several datasets (Table 2) were used to evaluate the hydrology, the carbon fluxes and the phenology simulated by ORCHIDEE. This comparison aims to determine whether the 11LAY gives a better representation of Amazonian hydrology and vegetation feedback.

15 3.2.1 Total soil Water Storage (TWS)

TWS is the integrated water amount stored on and below the land surface. In this study, we used the $1^\circ \times 1^\circ$ monthly GRACE dataset which originates from a mission mapping the Earth's gravity field, and from which monthly terrestrial water storage variations can be derived. We use the RL04 "ss201008" version (Bettadpur, 2012) produced by the University of Texas at Austin/Center for Space Research (CSR) and the GeoForschungsZentrum at Potsdam (GFZ), downloaded from the TELLUS website (<http://grace.jpl.nasa.gov/data/gracemonthlymassgridsland>). In order to compare the TWS simulated by ORCHIDEE to GRACE data, we calculated from ORCHIDEE outputs the sum of soil moisture, snow-pack (negligible in Amazonia), water on the canopy and the free water stored in the four water routing reservoirs. GRACE data cover the 10 yr period April 2002–July 2011 and are expressed as the difference in

[Title Page](#)

[Abstract](#)

[Introduction](#)

[Conclusions](#)

[References](#)

[Tables](#)

[Figures](#)

◀

▶

[Back](#)

[Close](#)

[Full Screen / Esc](#)

[Printer-friendly Version](#)

[Interactive Discussion](#)



Two soil hydrology formulations tested for the Amazon basin

M. Guimberteau et al.

[Title Page](#)[Abstract](#)[Introduction](#)[Conclusions](#)[References](#)[Tables](#)[Figures](#)[◀](#)[▶](#)[Back](#)[Close](#)[Full Screen / Esc](#)[Printer-friendly Version](#)[Interactive Discussion](#)

Evapotranspiration (ET) and Gross Primary Productivity (GPP)

The increased number of in situ ET measurements and more advanced satellite remote sensing algorithms now enable ET to be mapped at a global scale. These maps can be used to evaluate LSM performance (e.g. Mueller et al., 2011). For this study, 5 we use monthly ET estimates at $0.5^\circ \times 0.5^\circ$ resolution from Jung et al. (2010). This product (hereafter called “MTE-ET” (Model Tree Ensemble-EvapoTranspiration)) was derived from an empirical up-scaling of FLUXNET eddy-covariance measurements using a machine-learning algorithm called MTE. The FLUXNET global network collects continuous in situ measurements of land-surface fluxes. Data from 253 globally distributed flux towers (4 in the Amazon basin) were processed, corrected and combined 10 with monthly gridded global meteorological data and the remotely sensed fraction of absorbed photosynthetically active radiation (Advanced Very High Resolution Radiometer (AVHRR), Sea-viewing Wide Field-of-view Sensor (SeaWiFS) and MEdium Resolution Imaging Spectrometer (MERIS)). The MTE-ET product has already been used for the evaluation of coupled and uncoupled LSM simulations (Mueller et al., 2011) and contributed to the creation of global long-term records of the terrestrial water budget (Pan 15 et al., 2012).

Vegetation Gross Primary Production (GPP) quantifies the gross CO_2 flux taken up during photosynthesis. Jung et al. (2011) provided a global data-driven GPP product 20 (hereafter called “MTE-GPP”) using a similar algorithm to that used to give ET. We used GPP generated at a $0.5^\circ \times 0.5^\circ$ spatial resolution and a monthly temporal frequency from 1982 to 2008.

River discharge (Q)

River discharge data have been collected and harmonized by the ORE HYBAM project 25 (Cochonneau et al., 2006). The same database used by Guimbarteau et al. (2012a) is used here, but updated up to 2011. Six river gauging stations (Table 3), representative of the main sub-basins of the Amazon basin (Fig. 1), are used to evaluate river

GMDD

7, 73–129, 2014

Two soil hydrology
formulations tested
for the Amazon basin

M. Guimbarteau et al.

[Title Page](#)
[Abstract](#) [Introduction](#)
[Conclusions](#) [References](#)
[Tables](#) [Figures](#)
[◀](#) [▶](#)
[◀](#) [▶](#)
[Back](#) [Close](#)
[Full Screen / Esc](#)
[Printer-friendly Version](#)
[Interactive Discussion](#)



Two soil hydrology formulations tested for the Amazon basin

M. Guimberteau et al.

discharge simulation by ORCHIDEE. Óbidos (OBI) is the last gauging station before the mouth of the Amazon and is thus the most representative station to assess the average simulated river flow over the whole basin. The station Fazenda Vista Alegre (FVA) measures the discharge of the Madeira sub-basin, in the southern part of the Amazon basin. The Madeira sub-basin has the largest contributing area and provides nearly 15 % of the total river flow measured at Óbidos (Table 3). But the largest contribution comes from the western region, gauged at São Paulo de Olivença (SPO) on the Rio Solimões, where the average river flow is about 26 % of the total flow measured at Óbidos. The Negro sub-basin at Serrinha (SER) has the lowest area, but makes a large contribution to the total discharge due to the high precipitation. The two southeastern sub-basins of the Tapajós and the Xingu rivers, gauged at Itaituba (ITA) and Altamira (ALT) respectively, flow into the Amazon downstream of the Óbidos station (Fig. 1).

For each gauging station, we have estimated an empirical basin lag time as the delay between the peaks of precipitation and river discharge due to the time required for runoff to travel to the basin outlet. This lag depends on the basin characteristics (size, soil, geology, slope, land use...). The Amazon basin hydrograph exhibits a basin lag time of about four months mainly due to the large size of the basin and the long residence time of water in the floodplains. The basin lag is lower (about one month) in the smaller sub-basins such as the Tapajós and the Negro. For the purpose of water budget estimation, we use an equivalent runoff, Q^* , as the discharge Q time-series, back-shifted using the empirical lag.

Residual water balance (ΔS)

The water balance equation gives the change in soil water storage $\Delta\dot{S} = \frac{\Delta S}{\Delta t}$, the residual of $P - ET - Q^*$. It represents the amount of water that enters in the soil during the wet season ($\Delta\dot{S} > 0$) or is released ($\Delta\dot{S} < 0$) during the dry season. The mean annual change in storage is assumed to be negligible ($\Delta\dot{S} \approx 0$). However, inconsistencies between the different observation datasets could lead to a non-zero annual water storage

88

Two soil hydrology formulations tested for the Amazon basin

M. Guimberteau et al.

[Title Page](#)

[Abstract](#)

[Introduction](#)

[Conclusions](#)

[References](#)

[Tables](#)

[Figures](#)

[◀](#)

[▶](#)

[◀](#)

[▶](#)

[Back](#)

[Close](#)

[Full Screen / Esc](#)

[Printer-friendly Version](#)

[Interactive Discussion](#)



($\Delta S \neq 0$). The water closure condition is not fulfilled over the Solimões (bias of –25 %), the Xingu (–10 %) and the Negro (–6 %) sub-basins, probably due to the underestimated precipitation in the ORE HYBAM dataset over the western and north western sub-basins (Azarderakhsh et al., 2011; Guimberteau et al., 2012a) or to the low density of flux towers measuring ET over the Amazon basin in the MTE-ET product. For the Amazon, the Tapajós and the Madeira basins, the bias is between –5 and –2 %.

3.2.3 Leaf Area Index (LAI)

A Leaf Area Index (LAI) dataset is critical for monitoring global vegetation dynamics. For this study we use Zhu et al. (2013)'s product, based on a neural network algorithm which combines the third generation Global Inventory Modeling and Mapping Studies (GIMMS) Normalized Difference Vegetation Index (NDVI3g) and best-quality Terra Moderate Resolution Imaging Spectroradiometer (MODIS) LAI for the overlapping period 2000–2009. The global field of LAI was generated at 1/12° spatial resolution and a 15 day temporal frequency from 1982 to 2011. The comparison of the LAI with 45 sets of field measurements from 29 sites representative of all major biomes indicated a reasonable agreement ($p < 0.001$; RMSE = 0.68 LAI, Zhu et al., 2013).

3.3 Amplitude and phase assessment

To give an accurate estimate of the difference in TWS change between ORCHIDEE and GRACE, we use two indicators measuring the amplitude (α in mm) and the phase (ϕ in days) of the TWS seasonal cycles. The amplitude is defined as the difference between the monthly maximum and minimum values between January and December. The phase is computed by a fit to the cosine function as follows:

$$Y = p_0 + p_1 \cos\left(\frac{2\pi D}{365} - \frac{\phi_1 2\pi}{365}\right) + p_2 \cos\left(\frac{4\pi D}{365} - \frac{\phi_2 2\pi}{365}\right) + p_3 \cos\left(\frac{8\pi D}{365} - \frac{\phi_3 2\pi}{365}\right) \quad (1)$$

where Y is TWS (monthly average during 2003–2008), D is the day year, ϕ_1 , ϕ_2 and ϕ_3 are the phases of the seasonality, and p_0 , p_1 , p_2 and p_3 are regressed parameters. For the phase difference, only the phase of the first harmonics (ϕ_1 in Eq. 1) is considered here.

5 4 Results and discussion

4.1 Water budgets for the Amazon sub-basins

4.1.1 Overview of observed water budgets

Water budgets were first calculated from the different sets of observations: P (ORE HYBAM), ET (MTE-ET) and Q (ORE HYBAM) (Table 4). From these “observed” basin-level water budgets, the estimated precipitation amount over the Amazon basin is 6.2 mm d^{-1} . Half of this water runs off to the mouth (3.3 mm d^{-1}) and the other half evaporates (3.2 mm d^{-1}) in agreement with the estimates by Shuttleworth (1988) (based on on-site measured precipitation and ET estimated from a model calibrated against micro-meteorological measurements) and Callede et al. (2008) (based on precipitation and river discharge observations). Monthly precipitation averaged over the Amazon basin is between 3.5 mm d^{-1} in August and 8.2 mm d^{-1} in February (Fig. 2a). This is reflected in the western Solimões sub-basin (Fig. 2e), which receives 5.7 mm d^{-1} in annual precipitation (Table 4). The seasonal amplitude of precipitation is larger in the Madeira sub-basin (Fig. 2d) which includes southern tropical regions subject to the seasonal displacement of the Inter-Tropical Convergence Zone (ITCZ) during the year. The JJA dry season is particularly marked in the Xingu and Tapajós sub-basins in the southeast (Fig. 2b and c, respectively), with dry-season precipitation close to zero. By contrast, the DJF wet season precipitation for those sub-basins averages about 10.0 mm d^{-1} . The northern tropical sub-basin of the Rio Negro (Fig. 2f) receives



Two soil hydrology formulations tested for the Amazon basin

M. Guimberteau et al.

[Title Page](#)

[Abstract](#)

[Introduction](#)

[Conclusions](#)

[References](#)

[Tables](#)

[Figures](#)

◀

▶

[Back](#)

[Close](#)

[Full Screen / Esc](#)

[Printer-friendly Version](#)

[Interactive Discussion](#)



of annual MTE-ET ($\pm 13\%$) (see error bars in Fig. 1d for the bioclimatic zone “equatorial, fully humid” in Jung et al. (2010)). The underestimation in both ET and Q over the Solimões sub-basin suggests a disagreement between the evaluation datasets.

On average, the difference in simulated water budgets between the two soil models was small over the Amazon basin (about 3 %). However, the water budget was slightly improved with the 11LAY which systematically reduced the bias for each sub-basin (Table 4). Except for the Negro sub-basin where the values of ET and thus of Q are similar for both simulations, bias in annual ET was reduced by 3 to 4 % with the 11LAY, which simulated higher ET than the 2LAY. The overestimation in annual river discharge at the southern stations was consequently between 5 to 10 % less when using 11LAY than when using 2LAY. Contradictory effects on the bias of ET and Q by the two models over the Solimões sub-basin, result from the error in closure of the observed water balance.

4.2 Total water storage change and contribution from the different reservoirs

Seasonal (Sect. 4.2.1) and interannual (Sect. 4.2.2) variations in TWS from the two soil versions of ORCHIDEE are compared to the GRACE data over the Amazon basin and its sub-basins, during the 2003–2008 period.

4.2.1 Seasonal variation

The two different soil models simulate a similar TWS seasonal cycle over the entire Amazon basin (Fig. 3a and Table 5) with a half-monthly delay and an overestimated amplitude of about 30 and 56 mm compared to GRACE data (for the 2LAY and 11LAY, respectively). This positive amplitude bias was predominant along the Amazonian rivers (main stem of the Amazon and the Madeira, Tapajós and Xingu, Fig. 4a and b) suggesting the routing reservoir storages played a prevalent role in the overestimation of the TWS seasonal amplitude. TWS phase simulated by ORCHIDEE was overestimated (i.e. modeled TWS change occurred later than observed) by more than 25 days

[Title Page](#)[Abstract](#)[Introduction](#)[Conclusions](#)[References](#)[Tables](#)[Figures](#)[◀](#)[▶](#)[Back](#)[Close](#)[Full Screen / Esc](#)[Printer-friendly Version](#)[Interactive Discussion](#)

Two soil hydrology formulations tested for the Amazon basin

M. Guimbetteau et al.

[Title Page](#)[Abstract](#)[Introduction](#)[Conclusions](#)[References](#)[Tables](#)[Figures](#)[◀](#)[▶](#)[Back](#)[Close](#)[Full Screen / Esc](#)[Printer-friendly Version](#)[Interactive Discussion](#)

in the northern region of the Amazon basin and in the southern floodplain areas of the Madeira sub-basin (Fig. 4c and d). Underestimation (i.e. modeled TWS change occurred earlier than observed) by 20 days was also simulated in the Andes and in the two southern sub-basins (Tapajós and Xingu). Higher monthly correlation between 5 observed and simulated TWS was obtained with the 11LAY over the Amazon basin (Table 6). Storage increase during the early wet season was underestimated by the two models (50 mm in January and February) and the simulated TWS maximum in May was overestimated by 30 mm (Fig. 3a). 11LAY was better at representing the TWS decrease, leading to better capture of the timing of the TWS minima. More strikingly, the 10 five water storage reservoirs of the model contributed to TWS in a different way according which soil model was used. In both simulations, changes in the slow reservoir water content (in green in Fig. 3a) made the largest contribution to total TWS change. The annual amplitude in water storage in the slow reservoir storage was higher with the 2LAY (61 % of the total annual amplitude of TWS) than with the 11LAY (41 %). By 15 contrast, more water was stored in the soil (in blue in Fig. 3a) with the 11LAY (34 % compared to 24 % with the 2LAY). 11LAY drainage depends upon the soil water diffusion computation and the higher soil water holding capacity of the 11LAY enabled more water storage in the soil. The combination of these two effects led to a lower drainage contribution to the total runoff (43 %) compared to the 2LAY where the total soil water 20 excess giving runoff is partitioned arbitrarily into 95 % drainage and 5 % surface runoff. Thus, water in the 2LAY was primarily stored in the slow reservoir, which collects the drainage; while, because the 11LAY had more water storage in the soil reservoir, it produced a higher amplitude in the TWS seasonal cycle.

According to GRACE data, the southern sub-basins (Xingu, Tapajós and Madeira) 25 exhibit a pronounced TWS seasonal cycle (Fig. 3b–d), which is due to the high annual precipitation amplitude (see Sect. 4.1.1). This more pronounced TWS seasonal cycle in the south is well represented by ORCHIDEE which exhibited high seasonal correlation with GRACE ($0.96 < r^2 < 0.98$) (Table 6). When the seasonal cycle is removed from the time-series to reveal the interannual variability (IAV), the monthly correlation

Two soil hydrology formulations tested for the Amazon basin

M. Guimbeteau et al.

[Title Page](#)[Abstract](#)[Introduction](#)[Conclusions](#)[References](#)[Tables](#)[Figures](#)[◀](#)[▶](#)[Back](#)[Close](#)[Full Screen / Esc](#)[Printer-friendly Version](#)[Interactive Discussion](#)

strongly decreases in the Xingu and Tapajós sub-basins, suggesting that TWS IAV was difficult to capture (see Sect. 4.2.2). The simulated TWS amplitude was overestimated by between 45 to 195 mm in the three southern sub-basins (Table 5), while the phase was well captured by both models (difference between –10 to +8 days). The 11LAY

5 systematically produced a better amplitude when compared to GRACE in the three sub-basins, due to the larger storage of water in the soil reservoir (Fig. 3b–d). The amplitude was particularly improved in the southern part of the Tapajós and the northern part of the Xingu sub-basins (Fig. 4a and b). Phase improvement was obtained with the 11LAY in the southern parts of these two southeastern sub-basins (Fig. 4c and d).

10 The western Solimões sub-basin has the lowest TWS amplitude, which was well captured by ORCHIDEE – particularly by the 11LAY (Fig. 3e and Table 6). Here again, deseasonalized TWS anomalies are much lower (Table 6). The simulated TWS amplitude is overestimated by about 30 to 40 mm when compared to GRACE data, but lower bias occurs with the 11LAY. The phase was well captured by both models (Table 5), except in the Andes where it lagged by more than 25 days (Fig. 4).

15 The simulated TWS anomalies in the northern Negro sub-basin (Fig. 3f) exhibit low correlations with GRACE (Table 6) with a phase delay of more than one month and an underestimation of the amplitude by about 100 mm (Table 5 and Fig. 4). Here again, compared with the 2LAY, 11LAY reduced the bias by 34 mm and 7 days in amplitude and phase, respectively. For both soil models, the beginning of the storage period was delayed and the depletion exhibited too slow a decrease of stored water (Fig. 3f) relative to the GRACE data. The slow reservoir made a large contribution to the TWS seasonal cycle over the northern and western sub-basin in both schemes indicating that deep drainage was prevailing in these soils, in agreement with the results of Miguez-Macho and Fan (2012a). The underestimated amplitude of the simulated TWS compared to GRACE over the Negro sub-basin could be explained by the negative bias in the precipitation forcing dataset. Using satellite data products, Azarderakhsh et al. (2011) estimated from the water balance equation, that precipitation over the western and northwestern regions could be underestimated by up to 3.2 mm d^{-1} .

4.2.2 Interannual variation (IAV)

Using the deseasonalized TWS time series for the period 2003–2008 reveals the IAV in modeled TWS anomaly predicted by the two soil models in comparison to GRACE data. Figure 5 a shows the observed TWS averaged over the entire Amazon basin. It 5 reveals that the three first years are drier than the 2003–2008 average, while the last three years are wetter than average. This pattern agrees with Sheffield's precipitation anomaly variation. The TWS drop in GRACE during the intense drought of 2005 is due to the persistent negative monthly anomaly of precipitation during the year. The 10 abrupt increase of rainfall anomaly at the end of 2005 (-0.5 mm d^{-1} in November to $+1.5 \text{ mm d}^{-1}$ in December) and the persistent high positive anomaly in precipitation in January ($+1.25 \text{ mm d}^{-1}$) led to a TWS positive anomaly at the beginning of 2006.

The simulated TWS anomaly variation over the Amazon basin is closer to GRACE data with the 11LAY than with the 2LAY (Table 6), particularly during the negative anomaly period from mid-2004 until the beginning of 2006 (Fig. 5a). The 2005 drought 15 is captured by ORCHIDEE but with too large a decrease in TWS at the end of the year, especially in the 2LAY (TWS lower than observed at the end of the year by up to -125 mm). ORCHIDEE simulated a positive wet anomaly overestimated by about 100 mm at the beginning of 2008, but bias was lower (80 mm) with 11LAY. Similar patterns occurred in the Madeira sub-basin but with less amplitude (Fig. 5d). The south- 20 eastern sub-basins (Xingu and Tapajós, Fig. 5b and c, respectively) exhibited higher abrupt transitions in TWS than the Madeira sub-basin, during the entire studied period. GRACE shows high increases in positive TWS anomaly (by up to $+200 \text{ mm}$ in the beginning of 2004) associated with intense precipitation events (up to $+4.0 \text{ mm d}^{-1}$). These mainly occurred at the beginning of 2004 and 2006 for the Xingu, and in 2006 25 and 2008 for the Tapajós. These events were not well captured by either soil model, except for 2004 in the Xingu. Overall, the TWS increase in 2008 was systematically overestimated by ORCHIDEE in the southern sub-basins. Low IAV of TWS measured by GRACE in the Solimões sub-basin (Fig. 5e) was overestimated by ORCHIDEE (up

[Title Page](#)[Abstract](#)[Introduction](#)[Conclusions](#)[References](#)[Tables](#)[Figures](#)[◀](#)[▶](#)[Back](#)[Close](#)[Full Screen / Esc](#)[Printer-friendly Version](#)[Interactive Discussion](#)

to +100 mm with the 2LAY). However, 11LAY reduced the bias leading to better correlation with GRACE (Table 6). Improvement particularly occurred from mid-2006 to the end of 2007 where 11LAY bias decreased by up to 30 mm. By contrast, the Negro sub-basin depicted high IAV of TWS (Fig. 5f). When compared to GRACE data, 5 ORCHIDEE estimates captured the intense dry events (anomalies of up to -100 mm in TWS) during the beginning of 2004 and mid-2005, but overestimated them by more than 70 mm in early 2005 and 2007.

Overall, the 11LAY provided similar TWS variation to the 2LAY but reduced the bias with GRACE in the Amazon sub-basins. Note that the introduction of a more process-10 based soil hydrology model did not degrade the overall model-data agreement – an achievement that should not be overlooked.

4.3 Spatial patterns and seasonal variations of ET and river discharge

Both soil models simulated similar spatial patterns in annual ET over the basin (thus, only shown for the 11LAY in Fig. 6a), with the highest ET ($> 3.5 \text{ mm d}^{-1}$) over the flood-15 plains near the mouth of the Amazon, and along the Guaporé and Mamoré rivers in the southern region (see Fig. 1 for the location of the rivers). The 11LAY gave higher annual ET than 2LAY in the southern regions (southern parts of the Madeira, Tapajós and Xingu sub-basins), in the Andes, near the mouth of the Amazon and in the north-20 ernmost part of the basin (between $+0.1$ and $+0.7 \text{ mm d}^{-1}$, Fig. 6c) whereas very few regions exhibited higher annual ET with the 2LAY. Simulated ET was strongly underes-25 timated when compared to MTE-ET, in the foothills of the eastern Andes ($> 1.0 \text{ mm d}^{-1}$) and, too a lesser degree, in the center of the basin (between -0.4 and -0.7 mm d^{-1} , Fig. 6e). By contrast, simulated ET was overestimated in floodplain areas (up to more than 1.0 mm d^{-1} , Fig. 6e). However, the MTE-ET product does not take into account floodplain areas and might underestimate actual ET. The largest difference in ET be-25tween the two soil models occurred during the end of the dry season (JAS) in the southeast of the Amazon basin (Fig. 6d). The southern part of the Xingu sub-basin exhibited a dry-season ET of about 4.0 mm d^{-1} with 11LAY (Fig. 6b), 1.0 mm d^{-1} higher

[Title Page](#)[Abstract](#)[Introduction](#)[Conclusions](#)[References](#)[Tables](#)[Figures](#)[◀](#)[▶](#)[Back](#)[Close](#)[Full Screen / Esc](#)[Printer-friendly Version](#)[Interactive Discussion](#)

than with 2LAY (Fig. 6d). 11LAY overestimated the ET by 0.5 mm d^{-1} in this region when compared to MTE-ET (Fig. 6f). We will further investigate the effect of soil water storage parameterization on dry-season ET over the Xingu sub-basin in Sect. 4.4.

The dry-season ET increase simulated by the 11LAY is also apparent in the seasonal cycles of ET over the Xingu and Tapajós sub-basins in Fig. 7b and c, respectively. In the other sub-basins, both soil models provided similar seasonal cycles (Fig. 7d–f). By means of water conservation (precipitation is the same for both simulations), the higher ET with the 11LAY results in river discharge decreases during the recession limb in the Xingu and Tapajós sub-basins (Fig. 7b and c, respectively), leading to better agreement with the ORE HYBAM data.

4.4 Dry-season evapotranspiration: case study of the Xingu sub-basin

The largest impact of the soil hydrology parameterization on ET and river discharge occurred for the Xingu and Tapajós sub-basins, in the southeastern region of the Amazon basin. The Xingu sub-basin, chosen as a case study in this section, is characterized by the existence of a marked dry season with low rainfall in JJA (Fig. 8a). During this season, the land surface receives less than 5 % of the annual total precipitation, with monthly precipitation that does not exceed 2.0 mm d^{-1} (yellow bands in Fig. 8a). The dry season is between two transition periods in MAM (and SON), where precipitation falls (rises) abruptly, by about 6.0 mm d^{-1} . The wet season occurs in DJF and brings 10.6 mm d^{-1} of precipitation on average.

On average, over the 2003–2008 period, the MTE-ET product shows rather flat ET variation when compared to the model results (Fig. 8b). Lowest MTE-ET mainly occurs after the wet season whereas it is higher during the dry season with the maximum occurring during the transition period when precipitation increases (SON). This is consistent with GRACE observations, showing a TWS increase during the transition period onset in September, an abrupt increase during the DJF wet season and a maximum value in MAM (Fig. 8c). Both soil models simulated similar ET variation during the rainy

[Title Page](#)[Abstract](#)[Introduction](#)[Conclusions](#)[References](#)[Tables](#)[Figures](#)[◀](#)[▶](#)[Back](#)[Close](#)[Full Screen / Esc](#)[Printer-friendly Version](#)[Interactive Discussion](#)

Two soil hydrology formulations tested for the Amazon basin

M. Guimberteau et al.

[Title Page](#)

[Abstract](#)

[Introduction](#)

[Conclusions](#)

[References](#)

[Tables](#)

[Figures](#)

◀

▶

[Back](#)

[Close](#)

[Full Screen / Esc](#)

[Printer-friendly Version](#)

[Interactive Discussion](#)



Two soil hydrology formulations tested for the Amazon basin

M. Guimbertea et al.

[Title Page](#)[Abstract](#)[Introduction](#)[Conclusions](#)[References](#)[Tables](#)[Figures](#)[◀](#)[▶](#)[◀](#)[▶](#)[Back](#)[Close](#)[Full Screen / Esc](#)[Printer-friendly Version](#)[Interactive Discussion](#)

4.5 Evapotranspiration sensitivity to dry season length

The 11LAY model simulated more ET than the 2LAY during the dry season, over the Amazon basin. To test the sensitivity of the two soil models to dry season duration, we defined the dry-season length (DSL) as the mean annual number of months with $P < 2.0 \text{ mm d}^{-1}$ over the time period 1980–2008. Using an alternative definition which took into account only consecutive months with $P < 2.0 \text{ mm d}^{-1}$ did not change the results. Representing ET variation from the two soil models as a function of the DSL over the whole Amazon (Fig. 10a) shows that the maximum ET was simulated by ORCHIDEE when the dry season was 4 months. A DSL of less than 4 months applies to 70 % of the total grid cells over the Amazon basin. When DSL is between 4 and 7 months, ET decrease is more pronounced with 2LAY than 11LAY. The maximum difference between the two models was with a DSL is of 5 months ($+0.45 \text{ mm d}^{-1}$, Fig. 10b), which applies to only 5 % of the total grid cells (Fig. 10a). For longer dry seasons (DSL > 7 months, for 5 % of the total grid-cells), the impact of soil model parameterization on ET was negligible.

Figure 10b highlights the differences in ET components which contribute to the total ET and LAI differences between the two soil models when DSL increases. For short dry seasons (DSL < 4 months), 11LAY estimated higher bare soil evaporation ($+0.07 \text{ mm d}^{-1}$) when compared to the 2LAY. The 11LAY water content in the very thin first layer was directly evaporated to satisfy the climatic demand. By contrast, the resistance to bare soil evaporation in the superficial layer of the 2LAY limited the water exchange. The 11LAY transpiration was consequently smaller than that estimated by the 2LAY. Evaporation of water intercepted by the canopy was the main ET component ($+0.05 \text{ mm d}^{-1}$) contributing to ET increase with the 11LAY when DSL takes values of less than 4 months.

For a longer dry season (4 and 5 months), bare soil evaporation continued to increase (up to $+0.25 \text{ mm d}^{-1}$) and lower water stress with the 11LAY (as reported in Sect. 4.4) led to enhanced transpiration of the same magnitude, increasing canopy



leaf area (up to +0.4 of LAI, Fig. 10b). For grid cells with a DSL between 6 and 10 months, neither of the models could supply ET because this period of water stress is too long. Under these conditions, transpiration (and LAI) difference between the two soil models decreases. Bare soil evaporation was still higher with the 11LAY (around $+0.25 \text{ mm d}^{-1}$), whereas difference in evaporation by interception loss decreased with decreasing LAI difference. Total ET remained higher with the 11LAY until a DSL of about 10 months. However, transpiration with the 2LAY became higher when DSL was greater than 7 months.

For extreme DSL (> 7 months), which applies to only a few grid cells over the domain (Fig. 10a), the soil water column was never saturated. Under these conditions, the higher water holding capacity of the 11LAY compared to the 2LAY no longer had any effect on ET supply. Moreover, the drainage flux, which is prescribed in the deepest soil layer of the 11LAY, decreased the residence time of the water in the soil column compared to the 2LAY where drainage flux does not exist. Water stress consequently became higher in the 11LAY leading to lower transpiration (up to -0.2 mm d^{-1}) and lower LAI (up to -0.4). Total ET became lower with the 11LAY when DSL was greater than 10 months; the difference in bare soil evaporation between soil models then decreased.

5 Conclusions

The availability of two soil hydrology models in ORCHIDEE created an opportunity to test the different impacts of these models on the estimated Amazonian water budget at the scale of the major tributary sub-basins and, for the first time, on carbon flux dynamics. Over the entire basin, the differences in the water budget components between the two soil models were small. The sub-basin scale study did not reveal any large annual differences between the models. Although the differences are small (around 5 %), the 11 layer soil diffusion scheme did reduce the bias in the estimates of ET (up to -4%) and Q (up to -10%), mainly in the southern sub-basins. The main difference between

Title Page	
Abstract	Introduction
Conclusions	References
Tables	Figures
◀	▶
◀	▶
Back	Close
Full Screen / Esc	
Printer-friendly Version	
Interactive Discussion	

the soil models lies in the water reservoir contribution to TWS. The higher water holding capacity in 11LAY allows more water to be stored in the soil and its physically based partitioning of runoff and drainage results in better estimates of ET sustainability and TWS variations. The 2LAY parameterization leads to most of the water being stored in the slow routing reservoir, which does not interact directly with the atmosphere and thus does not allow ET to occur from stored water. This difference in parameterization particularly affects ET during the dry season in the southern Xingu sub-basin. The 11LAY can sustain ET for three consecutive dry months; whereas the 2LAY limits it when the dry season is too long. Lower water stress in the 11LAY gave a better representation of the decrease in carbon fluxes during the dry season, limiting the LAI variation. Overall, our study highlights the dominant effect of the dry-season length on ET, vegetation phenology and carbon dynamics over the Amazon basin. More attention should be paid to improving the representation of the soil hydrology and the relationship between water-stress and vegetation dynamics in LSMs. Developing these relationships would improve our ability to simulate feedbacks on dry-season precipitation, and thus on low river flows which could severely decrease in the future over southern Amazonia (Guimberteau et al., 2013).

Our study suggests that soil moisture plays an important role in those regions of Amazonia that have strong seasonality in precipitation, with marked transition periods. This comparative study between the two soil models of ORCHIDEE is currently being extended to a global scale with the objective of identifying whether a signal can be found in the transition zones identified by Koster et al. (2004a), where soil moisture is expected to influence precipitation. From the perspective of the EU-FP7 AMAZALERT (Raising the alert about critical feedbacks between climate and long-term land-use change in the Amazon) project, the present work also emphasizes the need to improve the representation of the water-stress impact on carbon fluxes and vegetation dynamics, and the potential feedbacks these may have on Amazonian hydrology. Additional comparisons of site-level simulations with flux tower measurements across the basin would help to identify the main processes involved in water stress and lead to better

- [Title Page](#)
- [Abstract](#) [Introduction](#)
- [Conclusions](#) [References](#)
- [Tables](#) [Figures](#)
- [◀](#) [▶](#)
- [◀](#) [▶](#)
- [Back](#) [Close](#)
- [Full Screen / Esc](#)
- [Printer-friendly Version](#)
- [Interactive Discussion](#)



Two soil hydrology formulations tested for the Amazon basin

M. Guimbertea et al.

[Title Page](#)[Abstract](#)[Introduction](#)[Conclusions](#)[References](#)[Tables](#)[Figures](#)[◀](#)[▶](#)[Back](#)[Close](#)[Full Screen / Esc](#)[Printer-friendly Version](#)[Interactive Discussion](#)

understanding of the relationships between drought, the carbon cycle and phenology. The small improvement gained by using the 11 layer soil diffusion scheme on the Amazonian water budget should be further verified, particularly in areas where the forest has deep roots. We suspect that soil depth, and specifically rooting depth, should be extended to greater values than 2 m because the deep roots observed by Nepstad et al. (1994) enable Amazonian vegetation to maintain dry-season ET (Verbeeck et al., 2011); this phenomenon is likely to have a significant impact on the climate (Kleidon and Heimann, 2000).

6 Code availability

- 10 The source code of the ORCHIDEE model can be obtained upon request (see <http://labex.ipsl.fr/orchidee/index.php/contact>). Documentation on the code including scientific and technical aspects, is available here: <https://forge.ipsl.jussieu.fr/orchidee/wiki/Documentation>.

15 *Acknowledgements.* This work was financially supported by the EU-FP7 AMAZALERT (Raising the alert about critical feedbacks between climate and long-term land-use change in the Amazon) project. We acknowledge the ORE HYBAM team that made available their precipitation and river flow datasets for the Amazon basin (<http://www.ore-hybam.org>). We gratefully acknowledge Martin Jung for access to the ET and GPP dataset and Bertrand Decharme for providing Sheffield's forcing dataset including precipitation correction by GPCC. Simulations 20 with ORCHIDEE were performed using computational facilities of the Institut du Développement et des Ressources en Informatique Scientifique (IDRIS, CNRS, France). Grateful acknowledgement for proofreading and correcting the English edition goes to John Gash.

References

- 25 Alkama, R., Decharme, B., Douville, H., Becker, M., Cazenave, A., Sheffield, J., Volodire, A., Tyteca, S., and Le Moigne, P.: Global evaluation of the ISBA-TRIP continental hydrological

Two soil hydrology formulations tested for the Amazon basin

M. Guimbertea et al.

[Title Page](#)

[Abstract](#)

[Introduction](#)

[Conclusions](#)

[References](#)

[Tables](#)

[Figures](#)

◀

▶

[Back](#)

[Close](#)

[Full Screen / Esc](#)

[Printer-friendly Version](#)

[Interactive Discussion](#)



- Chen, J., Wilson, C., Tapley, B., Yang, Z., and Niu, G.: 2005 drought event in the Amazon River basin as measured by GRACE and estimated by climate models, *J. Geophys. Res.-Sol. Ea.*, 114, B05404, doi:10.1029/2008JB006056, 2009. 77
- Chen, J., Wilson, C., and Tapley, B.: The 2009 exceptional Amazon flood and interannual terrestrial water storage change observed by GRACE, *Water Resour. Res.*, 46, W12526, doi:10.1029/2010WR009383, 2010. 77
- Cochonneau, G., Sondag, F., Guyot, J., Geraldo, B., Filizola, N., Fraizy, P., Laraque, A., Magat, P., Martinez, J., Noriega, L., Oliveira, E., Ordonez, J., Pombosa, R., Seyler, F., Sidgwick, J., and Vauchel, P.: The Environmental Observation and Research project, ORE HY-BAM, and the rivers of the Amazon basin, IAHS Press, 44–50, 2006. 87, 115
- Coe, M., Costa, M., and Howard, E.: Simulating the surface waters of the Amazon River basin: impacts of new river geomorphic and flow parameterizations, *Hydrol. Process.*, 22, 2542–2553, 2007. 76
- Cox, P., Betts, R., Bunton, C., Essery, R., Rowntree, P., and Smith, J.: The impact of new land surface physics on the GCM simulation of climate and climate sensitivity, *Clim. Dynam.*, 15, 183–203, 1999. 77
- Crowley, J. W., Mitrovica, J. X., Bailey, R. C., Tamisiea, M. E., and Davis, J. L.: Annual variations in water storage and precipitation in the Amazon Basin, *J. Geod.*, 82, 9–13, 2008. 77
- Da Rocha, H., Manzi, O., and Shuttleworth, J.: Evapotranspiration, *Geoph. Monog. Series*, 186, 261–272, 2009a. 78
- Da Rocha, H. R., Manzi, A. O., Cabral, O. M., Miller, S. D., Goulden, M. L., Saleska, S. R., R-Coupe, N., Wofsy, S. C., Borma, L. S., Artaxo, P., Vourlitis, G., Nogueira, J. S., Cardoso, F. L., Nobre, A. D., Kruijt, B., Freitas, H. C., von Randow, C., Aguiar, R. G., and Maia, J. F.: Patterns of water and heat flux across a biome gradient from tropical forest to savanna in Brazil, *J. Geophys. Res.-Biogeo.*, 114, G00B12, doi:10.1029/2007JG000640, 2009b. 78
- Dai, Y., Zeng, X., Dickinson, R. E., Baker, I., Bonan, G. B., Bosilovich, M. G., Denning, A. S., Dirmeyer, P. A., Houser, P. R., Niu, G., Oleson, K. W., Schlosser, C. A., and Zong-Liang, Y.: The common land model, *B. Am. Meteorol. Soc.*, 84, 1013–1023, 2003. 77
- de Rosnay, P. and Polcher, J.: Modelling root water uptake in a complex land surface scheme coupled to a GCM, *Hydrol. Earth Syst. Sci.*, 2, 239–255, doi:10.5194/hess-2-239-1998, 1998. 79, 80



Two soil hydrology formulations tested for the Amazon basin

M. Guimbertea et al.

[Title Page](#)

[Abstract](#)

[Introduction](#)

[Conclusions](#)

[References](#)

[Tables](#)

[Figures](#)

◀

▶

[Back](#)

[Close](#)

[Full Screen / Esc](#)

[Printer-friendly Version](#)

[Interactive Discussion](#)



- De Rosnay, P., Bruen, M., and Polcher, J.: Sensitivity of surface fluxes to the number of layers in the soil model used in GCMs, *Geophys. Res. Lett.*, 27, 3329–3332, doi:10.1029/2000GL011574, 2000. 77, 80, 81
- 5 De Rosnay, P., Polcher, J., Bruen, M., and Laval, K.: Impact of a physically based soil water flow and soil-plant interaction representation for modeling large-scale land surface processes, *J. Geophys. Res.-Atmos.*, 107, 4118, doi:10.1029/2001JD000634, 2002. 77, 80, 81, 82
- 10 De Weirdt, M., Verbeeck, H., Maignan, F., Peylin, P., Poulter, B., Bonal, D., Ciais, P., and Steppe, K.: Seasonal leaf dynamics for tropical evergreen forests in a process-based global ecosystem model, *Geosci. Model Dev.*, 5, 1091–1108, doi:10.5194/gmd-5-1091-2012, 2012. 99
- Decharme, B. and Douville, H.: Uncertainties in the GSWP-2 precipitation forcing and their impacts on regional and global hydrological simulations, *Clim. Dynam.*, 27, 695–713, 2006. 85
- 15 Decharme, B., Douville, H., Prigent, C., Papa, F., and Aires, F.: A new river flooding scheme for global climate applications: off-line evaluation over South America, *J. Geophys. Res.-Atmos.*, 113, D11110, doi:10.1029/2007JD009376, 2008. 76
- Decharme, B., Boone, A., Delire, C., and Noilhan, J.: Local evaluation of the Interaction between Soil Biosphere Atmosphere soil multilayer diffusion scheme using four pedotransfer functions, *J. Geophys. Res.-Atmos.*, 116, D20126, doi:10.1029/2011JD016002, 2011. 77
- 20 D'Orgeval, T.: Impact du changement climatique sur le cycle de l'eau en Afrique de l'Ouest: modélisation et incertitudes, Ph.D. thesis, Université Paris VI, 2006. 81, 83
- D'Orgeval, T., Polcher, J., and de Rosnay, P.: Sensitivity of the West African hydrological cycle in ORCHIDEE to infiltration processes, *Hydrol. Earth Syst. Sci.*, 12, 1387–1401, doi:10.5194/hess-12-1387-2008, 2008. 80, 81, 82, 84
- 25 Douville, H.: Relative contribution of soil moisture and snow mass to seasonal climate predictability: a pilot study, *Clim. Dynam.*, 34, 797–818, 2010. 77
- Ducharne, A., Laval, K., and Polcher, J.: Sensitivity of the hydrological cycle to the parametrization of soil hydrology in a GCM, *Clim. Dynam.*, 14, 307–327, 1998. 80
- 30 Ducharne, A., Golaz, C., Leblois, E., Laval, K., Polcher, J., Ledoux, E., and de Marsily, G.: Development of a high resolution runoff routing model, calibration and application to assess runoff from the LMD GCM, *J. Hydrol.*, 280, 207–228, 2003. 83

Two soil hydrology formulations tested for the Amazon basin

M. Guimberteau et al.

- Ducoudré, N., Laval, K., and Perrier, A.: SECHIBA, a new set of parameterizations of the hydrologic exchanges at the land atmosphere interface within the LMD atmospheric global circulation model, *J. Climate*, 6, 248–273, 1993. 79, 80

Dunne, T. and Black, R. D.: An experimental investigation of runoff production in permeable soils, *Water Resour. Res.*, 6, 478–490, 1970. 81

Entekhabi, D., Rodriguez-Iturbe, I., and Castelli, F.: Mutual interaction of soil moisture state and atmospheric processes, *J. Hydrol.*, 184, 3–17, 1996. 99

Famiglietti, J. S.: Remote sensing of terrestrial water storage, in: *Soil Moisture and Surface Waters*, vol. 150, American Geophysical Union, Washington, D.C., 197–207, 2004. 76

Fan, Y. and Miguez-Macho, G.: Potential groundwater contribution to Amazon evapotranspiration, *Hydrol. Earth Syst. Sci.*, 14, 2039–2056, doi:10.5194/hess-14-2039-2010, 2010. 76

FAO: Soil map of the world, scale 1 : 5000000, Tech. rep., United Nations, volumes I–X, United Nations Educationnal, Scientific and Cultural Organization, Paris, 1978. 81

Fekete, B., Vörösmarty, C., and Grabs, W.: Global, Composite Runoff Fields Based on Observed River Discharge and Simulated Water Balances, Tech. rep., Global Runoff Data Centre, Koblenz, Germany, 1999. 83

Frappart, F., Papa, F., Famiglietti, J. S., Prigent, C., Rossow, W. B., and Seyler, F.: Interannual variations of river water storage from a multiple satellite approach: a case study for the Rio Negro River basin, *J. Geophys. Res.-Atmos.*, 113, D21104, doi:10.1029/2007JD009438, 2008. 77

Frappart, F., Papa, F., Güntner, A., Werth, S., Santos da Silva, J., Tomasella, J., Seyler, F., Prigent, C., Rossow, W. B., Calmant, S., and Bonnet, M.-P.: Satellite-based estimates of groundwater storage variations in large drainage basins with extensive floodplains, *Remote Sens. Environ.*, 115, 1588–1594, 2011. 77

Frappart, F., Papa, F., Da Silva, J. S., Ramillien, G., Prigent, C., Seyler, F., and Calmant, S.: Surface freshwater storage and dynamics in the Amazon basin during the 2005 exceptional drought, *Environ. Res. Lett.*, 7, 044010, doi:10.1088/1748-9326/7/4/044010, 2012. 77

Frappart, F., Ramillien, G., and Ronchail, J.: Changes in terrestrial water storage vs. rainfall and discharges in the Amazon basin, *Int. J. Climatol.*, 33, 3029–3046, 2013. 77

Garrigues, S., Lacaze, R., Baret, F., Morisette, J., Weiss, M., Nickeson, J., Fernandes, R., Plummer, S., Shabanov, N., Myneni, R., Knyazikhin, Y., and Yang, W.: Validation and intercomparison of global Leaf Area Index products derived from remote sensing data, *J. Geophys. Res.-Biogeo.*, 113, G02028, doi:10.1029/2007JG000635, 2008. 99



Getirana, A., Bonnet, M., Rotunno Filho, O., Collischonn, W., Guyot, J., Seyler, F., and Mansur, W.: Hydrological modelling and water balance of the Negro River basin: evaluation based on in situ and spatial altimetry data, *Hydrol. Process.*, 24, 3219–3236, 2010. 76

Green, W. H. and Ampt, G.: Studies on soil physics, 1. The flow of air and water through soils, *J. Agr. Sci.*, 4, 1–24, 1911. 82

Guillod, B. P., Davin, E. L., Kündig, C., Smiatek, G., and Seneviratne, S. I.: Impact of soil map specifications for European climate simulations, *Clim. Dynam.*, 40, 123–141, 2013. 77

Guimbarteau, M., Drapeau, G., Ronchail, J., Sultan, B., Polcher, J., Martinez, J.-M., Prigent, C., Guyot, J.-L., Cochonneau, G., Espinoza, J. C., Filizola, N., Fraizy, P., Lavado, W., De Oliveira, E., Pombosa, R., Noriega, L., and Vauchel, P.: Discharge simulation in the sub-basins of the Amazon using ORCHIDEE forced by new datasets, *Hydrol. Earth Syst. Sci.*, 16, 911–935, doi:10.5194/hess-16-911-2012, 2012a. 76, 81, 83, 84, 86, 87, 89, 91, 115, 120

Guimbarteau, M., Perrier, A., Laval, K., and Polcher, J.: A comprehensive approach to analyze discrepancies between land surface models and in-situ measurements: a case study over the US and Illinois with SECHIBA forced by NLDAS, *Hydrol. Earth Syst. Sci.*, 16, 3973–3988, doi:10.5194/hess-16-3973-2012, 2012b. 80

Guimbarteau, M., Ronchail, J., Espinoza, J., Lengaigne, M., Sultan, B., Polcher, J., Drapeau, G., Guyot, J., Ducharne, A., and Ciais, P.: Future changes in precipitation and impacts on extreme streamflow over Amazonian sub-basins, *Environ. Res. Lett.*, 8, 014035, doi:10.1088/1748-9326/8/1/014035, 2013. 78, 81, 102

Hagemann, S. and Dumenil, L.: A parameterization of the lateral waterflow for the global scale, *Clim. Dynam.*, 14, 17–31, 1998. 83

Horton, R. E.: The role of infiltration in the hydrologic cycle, *Trans. Am. Geophys. Union*, 14, 446–460, 1933. 82

Huffman, G., Adler, R., Morrissey, M., Bolvin, D., Curtis, S., Joyce, R., McGavock, B., and Susskind, J.: Global precipitation at one-degree daily resolution from multisatellite observations, *J. Hydrometeorol.*, 2, 36–50, 2001. 84

Huffman, G., Bolvin, D., Nelkin, E., Wolff, D., Adler, R., Gu, G., Hong, Y., Bowman, K., and Stocker, E.: The TRMM multisatellite precipitation analysis (TMPA): quasi-global, multiyear, combined-sensor precipitation estimates at fine scales, *J. Hydrometeorol.*, 8, 38–55, 2007. 84

Jin, S. and Feng, G.: Large-scale global groundwater variations from satellite gravimetry and hydrological models, 2002–2012, *Global Planet. Change*, 106, 20–30, 2013. 76

Two soil hydrology formulations tested for the Amazon basin

M. Guimbarteau et al.

[Title Page](#)

[Abstract](#)

[Introduction](#)

[Conclusions](#)

[References](#)

[Tables](#)

[Figures](#)

◀

▶

◀

▶

[Back](#)

[Close](#)

[Full Screen / Esc](#)

[Printer-friendly Version](#)

[Interactive Discussion](#)



- 5 Jung, M., Reichstein, M., Ciais, P., Seneviratne, S., Sheffield, J., Goulden, M., Bonan, G., Cescatti, A., Chen, J., De Jeu, R., Johannes Dolman, A., Eugster, W., Gerten, D., Gianelle, D., Gobron, N., Heinke, J., Kimball, J., Law, B. E., Montagnani, L., Mu, Q., Mueller, B., Oleson, K., Papale, D., Richardson, A. D., Roupsard, O., Running, S., Tomelleri, E., Viovy, N., Weber, U., Williams, C., Wood, E., Zaehle, S., and Zhang, K.: Recent decline in the global land evapotranspiration trend due to limited moisture supply, *Nature*, 467, 951–954, 2010. 87, 92, 115
- 10 Jung, M., Reichstein, M., Margolis, H., Cescatti, A., Richardson, A., Arain, M., Arneth, A., Bernhofer, C., Bonal, D., Chen, J., Gianelle, D., Gobron, N., Kiely, G., Kutsch, W., Lasslop, G., Law, B. E., Lindroth, A., Merbold, L., Montagnani, L., Moors, E. J., Papale, D., Sottocornola, M., Vaccari, F., and Williams, C.: Global patterns of land–atmosphere fluxes of carbon dioxide, latent heat, and sensible heat derived from eddy covariance, satellite, and meteorological observations, *J. Geophys. Res.-Biogeo.*, 116, G00J07, doi:10.1029/2010JG001566, 2011. 87, 115
- 15 Kistler, R., Kalnay, E., Collins, W., Saha, S., White, G., Woollen, J., Chelliah, M., Ebisuzaki, W., Kanamitsu, M., Kousky, V., van den Dool, H., Jenne, R., and Fiorino, M.: The NCEP-NCAR 50 yr reanalysis: monthly means CD-ROM and documentation, *B. Am. Meteorol. Soc.*, 82, 247–267, 2001. 84
- 20 Kleidon, A. and Heimann, M.: Assessing the role of deep rooted vegetation in the climate system with model simulations: mechanism, comparison to observations and implications for Amazonian deforestation, *Clim. Dynam.*, 16, 183–199, 2000. 103
- 25 Koster, R., Dirmeyer, P., Guo, Z., Bonan, G., Chan, E., Cox, P., Gordon, C., Kanae, S., Kowalczyk, E., Lawrence, D., Liu, P., Lu, C., Malyshev, S., McAvaney, B., Mitchell, K., Mocko, D., Oki, T., Oleson, K., Pitman, A., Sud, Y., Taylor, C., Verseghy, D., Vasic, R., Xue, Y., Yamada, T., and Team, G.: Regions of strong coupling between soil moisture and precipitation, *Science*, 305, 1138–1140, 2004a. 78, 102
- 30 Koster, R. D., Suarez, M. J., Liu, P., Jambor, U., Berg, A., Kistler, M., Reichle, R., Rodell, M., and Famiglietti, J.: Realistic initialization of land surface states: impacts on subseasonal forecast skill, *J. Hydrometeorol.*, 5, 1049–1063, 2004b. 77
- Krinner, G., Viovy, N., de Noblet-Ducoudre, N., Ogee, J., Polcher, J., Friedlingstein, P., Ciais, P., Sitch, S., and Prentice, I.: A dynamic global vegetation model for studies of the coupled atmosphere-biosphere system, *Global Biogeochem. Cy.*, 19, 1–33, 2005. 78

Two soil hydrology formulations tested for the Amazon basin

M. Guimbertea et al.

[Title Page](#)

[Abstract](#)

[Introduction](#)

[Conclusions](#)

[References](#)

[Tables](#)

[Figures](#)

◀

▶

[Back](#)

[Close](#)

[Full Screen / Esc](#)

[Printer-friendly Version](#)

[Interactive Discussion](#)



- Li, W., Fu, R., and Dickinson, R.: Rainfall and its seasonality over the Amazon in the 21st century as assessed by the coupled models for the IPCC AR4, *J. Geophys. Res.-Atmos.*, 111, D02111, doi:10.1029/2005JD006355, 2006. 78
- Li, W., Fu, R., Juárez, R., and Fernandes, K.: Observed change of the standardized precipitation index, its potential cause and implications to future climate change in the Amazon region, *Philos. T. R. Soc. B*, 363, 1767–1772, 2008. 78
- Manabe, S.: Climate and ocean circulation, I. Atmospheric circulation and hydrology of earths surface, *Mon. Weather Rev.*, 97, 739–774, 1969. 80
- Manning, R.: On the flow of water in open channels and pipes, *Trans. Inst. Civil Engrs. (Dublin, Ireland)*, 20, 179–207, 1895. 83
- Marengo, J.: On the hydrological cycle of the Amazon Basin: a historical review and current state-of-the-art, *Rev. Bras. Meterol.*, 21, 1–19, 2006. 77
- McMurtrie, R., Rook, D., and Kelliher, F.: Modelling the yield of *Pinus radiata* on a site limited by water and nitrogen, *Forest Ecol. Manag.*, 30, 381–413, 1990. 82
- McNab, A. L.: Climate and drought, *Trans. Am. Geophys. Union*, 70, 873–883, 1989. 99
- Miguez-Macho, G. and Fan, Y.: The role of groundwater in the Amazon water cycle: 1. Influence on seasonal streamflow, flooding and wetlands, *J. Geophys. Res.-Atmos.*, 117, D15113, doi:10.1029/2012JD017539, 2012a. 76, 94
- Miguez-Macho, G. and Fan, Y.: The role of groundwater in the Amazon water cycle: 2. Influence on seasonal soil moisture and evapotranspiration, *J. Geophys. Res.-Atmos.*, 117, D15114, doi:10.1029/2012JD017540, 2012b. 76
- Miller, J., Russell, G., and Caliri, G.: Continental-scale river flow in climate models, *J. Climate*, 7, 914–928, 1994. 83
- Molinier, M. and Guyot, J.: Les régimes hydrologiques de l'Amazone et de ses affluents, *IAHS P.*, 238, 209–222, 1996. 76
- Mualem, Y.: A new model for predicting the hydraulic conductivity of unsaturated porous media, *Water Resour. Res.*, 12, 513–522, 1976. 81
- Mueller, B., Seneviratne, S., Jimenez, C., Corti, T., Hirschi, M., Balsamo, G., Ciais, P., Dirmeyer, P., Fisher, J., Guo, Z Jung, M., Maignan, F., McCabe, M. F., Reichle, R., Reichstein, M., Rodell, M., Sheffield, J., Teuling, A. J., Wang, K., Wood, E. F., and Zhang, Y.: Evaluation of global observations-based evapotranspiration datasets and IPCC AR4 simulations, *Geophys. Res. Lett.*, 38, L06402, doi:10.1029/2010GL046230, 2011. 87

[Title Page](#)[Abstract](#)[Introduction](#)[Conclusions](#)[References](#)[Tables](#)[Figures](#)[◀](#)[▶](#)[Back](#)[Close](#)[Full Screen / Esc](#)[Printer-friendly Version](#)[Interactive Discussion](#)

Two soil hydrology formulations tested for the Amazon basin

M. Guimberteau et al.

[Title Page](#)

[Abstract](#)

[Introduction](#)

[Conclusions](#)

[References](#)

[Tables](#)

[Figures](#)

◀

▶

[Back](#)

[Close](#)

[Full Screen / Esc](#)

[Printer-friendly Version](#)

[Interactive Discussion](#)



Nepstad, D. C., de Carvalho, C. R., Davidson, E. A., Jipp, P. H., Lefebvre, P. A., Negreiros, G. H., da Silva, E. D., Stone, T. A., Trumbore, S. E., and Vieira, S.: The role of deep roots in the hydrological and carbon cycles of Amazonian forests and pastures, *Nature*, 372, 666–669, 1994. 103

5 New, M., Hulme, M., and Jones, P.: Representing twentieth-century space-time climate variability, Part II: Development of 1901–96 monthly grids of terrestrial surface climate, *J. Climate*, 13, 2217–2238, 2000. 84

10 Ngo-Duc, T., Laval, K., Ramillien, G., Polcher, J., and Cazenave, A.: Validation of the land water storage simulated by Organising Carbon and Hydrology in Dynamic Ecosystems (OR-CHIDEE) with Gravity Recovery and Climate Experiment (GRACE) data, *Water Resour. Res.*, 43, W04427, doi:10.1029/2006WR004941, 2007. 76, 83

Oki, T., Nishimura, T., and Dirmeyer, P.: Assessment of annual runoff from land surface models using Total Runoff Integrating Pathways (TRIP), *J. Meteorol. Soc. Jpn.*, 77, 235–255, 1999. 83

15 Olson, J., Watts, J., and Allison, L.: Carbon in live vegetation of major world ecosystems, Tech. rep., Oak Ridge National Laboratory, Oak Ridge, Tennessee, USA, 1983. 82

Paiva, R., Collischonn, W., and Tucci, C.: Large scale hydrologic and hydrodynamic modeling using limited data and a GIS based approach, *J. Hydrol.*, 406, 170–181, 2011. 76

20 Paiva, R. C. D., Collischonn, W., Bonnet, M. P., and de Gonçalves, L. G. G.: On the sources of hydrological prediction uncertainty in the Amazon, *Hydrol. Earth Syst. Sci.*, 16, 3127–3137, doi:10.5194/hess-16-3127-2012, 2012. 76

Pan, M., Sahoo, A. K., Troy, T. J., Vinukollu, R. K., Sheffield, J., and Wood, E. F.: Multisource estimation of long-term terrestrial water budget for major global river basins, *J. Climate*, 25, 3191–3206, 2012. 87

25 Polcher, J.: Les processus de surface à l'échelle globale et leurs interactions avec l'atmosphère, *Habilitation à diriger des recherches*, Université Paris VI, 2003. 76, 83

Ramillien, G., Famiglietti, J., and Wahr, J.: Detection of continental hydrology and glaciology signals from GRACE: a review, *Surv. Geophys.*, 29, 361–374, 2008. 76

Richards, L. A.: Capillary conduction of liquids through porous media, *Physics*, 1, 318–333, 1931. 81

Schmidt, R., Schwintzer, P., Flechtner, F., Reigber, C., Güntner, A., Döll, P., Ramillien, G., Cazenave, A., Petrovic, S., Jochmann, H., and Wünsch, J.: GRACE observations of changes in continental water storage, *Global Planet. Change*, 50, 112–126, 2006. 76

- Schmidt, R., Petrovic, S., Günther, A., Barthelmes, F., Wünsch, J., and Kusche, J.: Periodic components of water storage changes from GRACE and global hydrology models, *J. Geophys. Res.-Sol. Ea.*, 113, B08419, doi:10.1029/2007JB005363, 2008. 76
- Schneider, U., Becker, A., Finger, P., Meyer-Christoffer, A., Ziese, M., and Rudolf, B.: GPCC's new land surface precipitation climatology based on quality-controlled in situ data and its role in quantifying the global water cycle, *Theor. Appl. Climatol.*, 1–26, doi:10.1007/s00704-013-0860-x, 2013. 84
- Sheffield, J., Goteti, G., and Wood, E.: Development of a 50 yr high-resolution global dataset of meteorological forcings for land surface modeling, *J. Climate*, 19, 3088–3111, 2006. 84, 86
- Shuttleworth, W.: Evaporation from Amazonian rainforest, *Proc. R. Soc. London, Ser. B*, 233, 321–346, 1988. 77, 90
- Sitch, S., Smith, B., Prentice, I., Arneth, A., Bondeau, A., Cramer, W., Kaplan, J., Levis, S., Lucht, W., Sykes, M., Thonicke, K., and Venevsky, S.: Evaluation of ecosystem dynamics, plant geography and terrestrial carbon cycling in the LPJ dynamic global vegetation model, *Glob. Change Biol.*, 9, 161–185, 2003. 79
- Swenson, S. and Wahr, J.: Methods for inferring regional surface-mass anomalies from Gravity Recovery and Climate Experiment (GRACE) measurements of time-variable gravity, *J. Geophys. Res.-Sol. Ea.*, 107, 2193, doi:10.1029/2001JB000576, 2002. 86
- Swenson, S. and Wahr, J.: Post-processing removal of correlated errors in GRACE data, *Geophys. Res. Lett.*, 33, L08, doi:10.1029/2005GL025285, 2006. 86
- Swenson, S., Wahr, J., and Milly, P.: Estimated accuracies of regional water storage variations inferred from the Gravity Recovery and Climate Experiment (GRACE), *Water Resour. Res.*, 39, 1223, doi:10.1029/2002WR001808, 2003. 86
- Syed, T., Famiglietti, J., Chen, J., Rodell, M., Seneviratne, S., Viterbo, P., and Wilson, C.: Total basin discharge for the Amazon and Mississippi River basins from GRACE and a land-atmosphere water balance, *Geophys. Res. Lett.*, 32, L24404, doi:10.1029/2005GL024851, 2005. 77
- Syed, T. H., Famiglietti, J. S., Rodell, M., Chen, J., and Wilson, C. R.: Analysis of terrestrial water storage changes from GRACE and GLDAS, *Water Resour. Res.*, 44, W02433, doi:10.1029/2006WR005779, 2008. 76
- Thompson, S. L. and Pollard, D.: A global climate model (GENESIS) with a land-surface transfer scheme (LSX), Part I: Present climate simulation, *J. Climate*, 8, 732–761, 1995. 77

Two soil hydrology formulations tested for the Amazon basin

M. Guimberteau et al.

[Title Page](#)

[Abstract](#)

[Introduction](#)

[Conclusions](#)

[References](#)

[Tables](#)

[Figures](#)

◀

▶

[Back](#)

[Close](#)

[Full Screen / Esc](#)

[Printer-friendly Version](#)

[Interactive Discussion](#)



- Trigg, M., Wilson, M., Bates, P., Horritt, M., Alsdorf, D., Forsberg, B., and Vega, M.: Amazon flood wave hydraulics, *J. Hydrol.*, 374, 92–105, 2009. 76
- Van Genuchten, M. T.: A closed-form equation for predicting the hydraulic conductivity of unsaturated soils, *Soil Sci. Soc. Am. J.*, 44, 892–898, 1980. 81
- Verbeeck, H., Peylin, P., Bacour, C., Bonal, D., Steppe, K., and Ciais, P.: Seasonal patterns of CO₂ fluxes in Amazon forests: fusion of eddy covariance data and the ORCHIDEE model, *J. Geophys. Res.-Biogeosci.*, 116, G02018, doi:10.1029/2010JG001544, 2011. 103
- Viovy, N.: Interannuality and CO₂ sensitivity of the SECHIBA-BGC coupled SVAT-BGC model, *Phys. Chem. Earth*, 21, 489–497, 1996. 79
- Viterbo, P. and Beljaars, A. C.: An improved land surface parameterization scheme in the ECMWF model and its validation, *J. Climate*, 8, 2716–2748, 1995. 77
- Vörösmarty, C., Fekete, B., Meybeck, M., and Lammers, R.: Global system of rivers: its role in organizing continental land mass and defining land-to-ocean linkages, *Global Biogeochem. Cy.*, 14, 599–621, 2000. 83
- Wahr, J., Swenson, S., Zlotnicki, V., and Velicogna, I.: Time-variable gravity from GRACE: first results, *Geophys. Res. Lett.*, 31, L11501, doi:10.1029/2004GL019779, 2004. 86
- Xavier, L., Becker, M., Cazenave, A., Longuevergne, L., Llovel, W., and Filho, O. R.: Interannual variability in water storage over 2003–2008 in the Amazon Basin from GRACE space gravimetry, in situ river level and precipitation data, *Remote Sens. Environ.*, 114, 1629–1637, 2010. 77
- Yamazaki, D., Kanae, S., Kim, H., and Oki, T.: A physically based description of floodplain inundation dynamics in a global river routing model, *Water Resour. Res.*, 47, W04501, doi:10.1029/2010WR009726, 2011. 76
- Yamazaki, D., Lee, H., Alsdorf, D., Dutra, E., Kim, H., Kanae, S., and Oki, T.: Analysis of the water level dynamics simulated by a global river model: a case study in the Amazon River, *Water Resour. Res.*, 48, W09508, doi:10.1029/2012WR011869, 2012. 76
- Zhu, Z., Bi, J., Pan, Y., Ganguly, S., Anav, A., Xu, L., Samanta, A., Piao, S., Nemani, R. R., and Myneni, R. B.: Global data sets of vegetation leaf area index (LAI) 3g and Fraction of Photosynthetically Active Radiation (FPAR) 3g derived from Global Inventory Modeling and Mapping Studies (GIMMS) Normalized Difference Vegetation Index (NDVI3g) for the period 1981 to 2011, *Remote Sens.*, 5, 927–948, 2013. 89, 115
- Zobler, L.: A world soil file for global climate modeling, *Tech. Rep.* 87802, NASA, 1986. 81

Two soil hydrology formulations tested for the Amazon basin

M. Guimbertea et al.

[Title Page](#)[Abstract](#)[Introduction](#)[Conclusions](#)[References](#)[Tables](#)[Figures](#)[◀](#)[▶](#)[Back](#)[Close](#)[Full Screen / Esc](#)[Printer-friendly Version](#)[Interactive Discussion](#)

Two soil hydrology formulations tested for the Amazon basin

M. Guimberteau et al.

Table 1. List of atmospheric variables in the Princeton forcing data.

Name	Description	Units	Sources
T_{air}	Two-meter air temperature	K	NCEP–NCAR reanalysis/CRU TS3.0
Q_{air}	Two-meter air specific humidity	kg kg^{-1}	NCEP–NCAR reanalysis
Wind	Ten-meter wind speed	m s^{-1}	NCEP–NCAR reanalysis
P_{surf}	Surface pressure	Pa	NCEP–NCAR reanalysis
SW_{down}	Surface downward short wave flux	W m^{-2}	NCEP–NCAR reanalysis/NASA Langley SRB V3.0
LW_{down}	Surface downward long wave flux	W m^{-2}	NCEP–NCAR reanalysis/NASA Langley SRB V3.0
P	Precipitation rate	$\text{kg m}^{-2} \text{s}^{-1}$	GPCC

[Title Page](#)

[Abstract](#)

[Introduction](#)

[Conclusions](#)

[References](#)

[Tables](#)

[Figures](#)

◀

▶

[Back](#)

[Close](#)

[Full Screen / Esc](#)

[Printer-friendly Version](#)

[Interactive Discussion](#)



Two soil hydrology formulations tested for the Amazon basin

M. Guimberteau et al.

Table 2. List of evaluation datasets.

Variable	Dataset	Resolution		Coverage		References
		Spatial	Temporal	Spatial	Temporal	
TWS change <i>P</i> <i>Q</i>	GRACE	1.0°	Monthly	Global	2002–2011	Bettadpur (2012)
	ORE HYBAM	1.0°	Daily	Amazon basin	1980–2009	Guimberteau et al. (2012a)
	ORE HYBAM	Station	Monthly	Amazon basin (scattered)	1980–2011	Cochonneau et al. (2006)
ET GPP	MTE-ET	0.5°	Monthly	Global	1982–2008	Jung et al. (2010)
	MTE-GPP	0.5°	Monthly	Global	1982–2008	Jung et al. (2011)
LAI	GIMMS	(1/12)°	Half-monthly	Global	1982–2011	Zhu et al. (2013)

Two soil hydrology formulations tested for the Amazon basin

M. Guimberteau et al.

Table 3. List of ORE HYBAM gauging stations over the Amazon basin. Q_{mean} is the mean annual discharge from ORE HYBAM data, averaged over the period 1980–2008.

Station	River		Lat	Lon	Q_{mean} ($\text{m}^3 \text{s}^{-1}$)	Q_{mean} contribution at OBI (%)	Basin area (km^2)
Óbidos	OBI	Amazonas	-1.95	-55.30	179 263	100	4 680 000
Altamira	ALT	Xingu	-3.38	-52.14	7900	—	469 100
Itaituba	ITA	Tapajós	-4.24	-56.00	11 767	—	461 100
Fazenda Vista Alegre	FVA	Madeira	-4.68	-60.03	27 705	15	1 293 600
São Paulo de Olivença	SPO	Solimões	-3.45	-68.75	46 717	26	990 781
Serrinha	SER	Negro	-0.48	-64.83	16 363	9	291 100

[Title Page](#)[Abstract](#)[Introduction](#)[Conclusions](#)[References](#)[Tables](#)[Figures](#)[|◀](#)[▶|](#)[◀](#)[▶](#)[Back](#)[Close](#)[Full Screen / Esc](#)[Printer-friendly Version](#)[Interactive Discussion](#)

Two soil hydrology formulations tested for the Amazon basin

M. Guimberteau et al.

Table 4. Mean annual values (mm d^{-1}), and bias against the observations (in mm d^{-1} and % in brackets), of the water budget components simulated by 2LAY and 11LAY, for each sub-basin, averaged over the period 1980–2008. The bold values indicated the smallest bias between 2LAY and 11LAY for a given sub-basin.

Amazon (OBI)				Xingu (ALT)				Tapajós (ITA)				
P	ET	Q	Δs	P	ET	Q	Δs	P	ET	Q	Δs	
2LAY	6.1	2.6	3.5	0	5.4	2.8	2.6	0	5.7	2.7	3.0	0
11LAY		2.7	3.4	0		2.9	2.5	0		2.9	2.8	0
Obs	6.2	3.2	3.3	-0.3	5.4	3.4	1.5	+0.5	5.7	3.3	2.2	+0.2
Bias				Bias				Bias				
2LAY	-0.1 (-1.2)	-0.5 (-17)	+0.2 (+5)		0 (+0.1)	-0.6 (-17)	+1.1 (+79)		0 (0)	-0.6 (-18)	+0.8 (+34)	
11LAY		-0.5 (-15)	+0.1 (+3)			-0.5 (-13)	+1.0 (+69)			-0.4 (-15)	+0.6 (+29)	
Madeira (FVA)				Solimões (SPO)				Negro (SER)				
P	ET	Q	Δs	P	ET	Q	Δs	P	ET	Q	Δs	
2LAY	5.0	2.6	2.4	0	5.8	2.3	3.5	0	8.4	2.8	5.6	0
11LAY		2.8	2.2	0		2.4	3.4	0		2.8	5.6	0
Obs	5.2	3.2	1.8	+0.2	5.7	3.0	4.1	-1.4	8.7	3.3	4.9	+0.5
Bias				Bias				Bias				
2LAY	-0.2 (-3.2)	-0.5 (-17)	+0.6 (+28)		+0.1 (+2.4)	-0.7 (-24)	-0.6 (-14)		-0.3 (-3.0)	-0.5 (-15)	+0.7 (+15)	
11LAY		-0.4 (-13)	+0.4 (+21)			-0.6 (-20)	-0.7 (-16)			-0.5 (-14)	+0.7 (+15)	



Two soil hydrology formulations tested for the Amazon basin

M. Guimberteau et al.

Table 5. Amplitude ($\Delta\alpha$ in mm) and phase ($\Delta\phi$ in days) differences of TWS between simulations (2LAY and 11LAY) and GRACE, for each sub-basin, for the period 2003–2008. The bold values correspond to the lowest bias between 2LAY or 11LAY with GRACE for a given sub-basin.

Amazon		Xingu (ALT)		Tapajós (ITA)		Madeira (FVA)		Solimões (SPO)		Negro (SER)		
$\Delta\alpha$	$\Delta\phi$											
2LAY	+30	+15	+195	-6	+94	-10	+58	+3	+42	-3	-132	+43
11LAY	+56	+13	+152	-6	+61	-6	+45	+8	+26	-1	-98	+36

**Two soil hydrology
formulations tested
for the Amazon basin**

M. Guimberteau et al.

Table 6. Monthly correlation of TWS anomalies, between simulations (2LAY and 11LAY) and GRACE, over the Amazon basin and its sub-basins, for the period 2003–2008. Values between brackets indicate correlation of deseasonalized TWS anomalies. The bold values correspond to the highest correlation between 2LAY or 11LAY with GRACE for a given sub-basin.

	Amazon	Xingu (ALT)	Tapajós (ITA)	Madeira (FVA)	Solimões (SPO)	Negro (SER)
2LAY	0.91 (0.85)	0.97 (0.66)	0.97 (0.55)	0.98 (0.81)	0.84 (0.50)	0.70 (0.57)
11LAY	0.95 (0.90)	0.97 (0.61)	0.98 (0.56)	0.96 (0.77)	0.89 (0.60)	0.75 (0.58)

[Title Page](#)[Abstract](#)[Introduction](#)[Conclusions](#)[References](#)[Tables](#)[Figures](#)[Back](#)[Close](#)[Full Screen / Esc](#)[Printer-friendly Version](#)[Interactive Discussion](#)

Two soil hydrology formulations tested for the Amazon basin

M. Guimberteau et al.

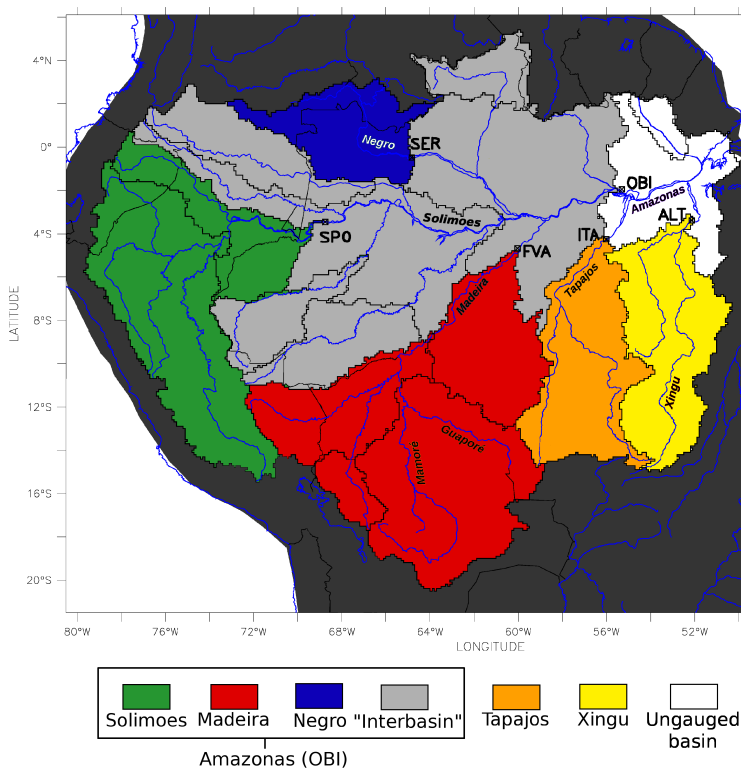


Fig. 1. Map of the Amazon sub-basins and their corresponding gauging stations. Color is used to indicate the sub-basins studied here. Modified from Guimberteau et al. (2012a).

[Title Page](#)[Abstract](#)[Introduction](#)[Conclusions](#)[References](#)[Tables](#)[Figures](#)[◀](#)[▶](#)[Back](#)[Close](#)[Full Screen / Esc](#)[Printer-friendly Version](#)[Interactive Discussion](#)

Two soil hydrology formulations tested for the Amazon basin

M. Guimbeteau et al.

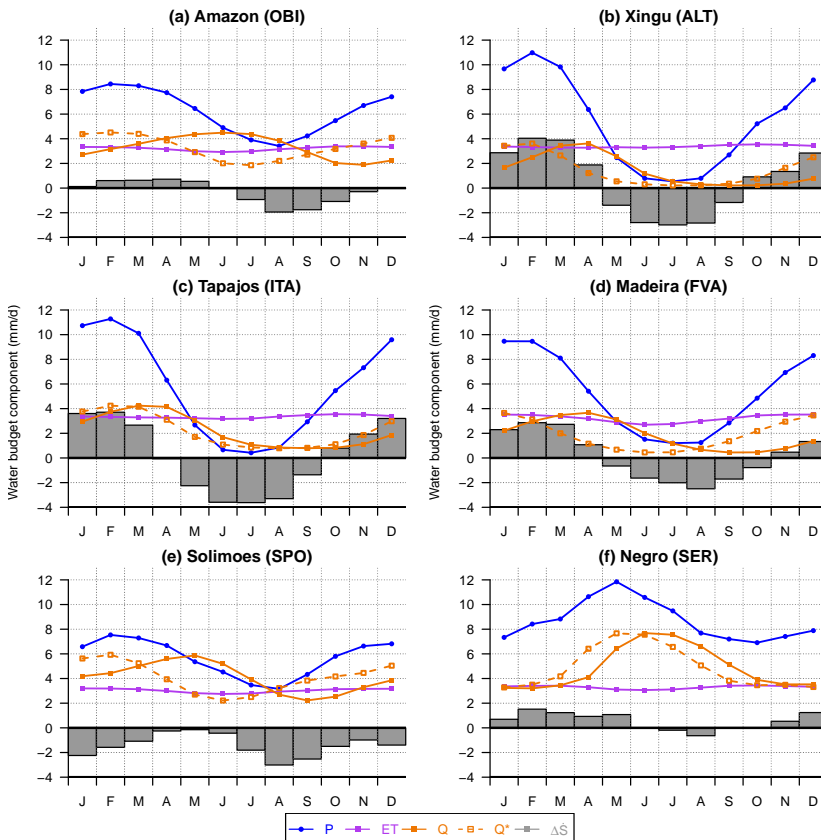


Fig. 2. Monthly mean seasonalities of the water budget components (mm d^{-1}) from observations, for each sub-basin, averaged over the period 1980–2008. Q^* is the equivalent runoff as the discharge Q time-series, back-shifted using the empirical lag. The change in soil water storage ΔS is estimated as residual of $P - ET - Q^*$.

Printer-friendly Version

Interactive Discussion

- [Title Page](#)
- [Abstract](#) [Introduction](#)
- [Conclusions](#) [References](#)
- [Tables](#) [Figures](#)
- [◀](#) [▶](#)
- [◀](#) [▶](#)
- [Back](#) [Close](#)
- [Full Screen / Esc](#)

Two soil hydrology formulations tested for the Amazon basin

M. Guimberteau et al.

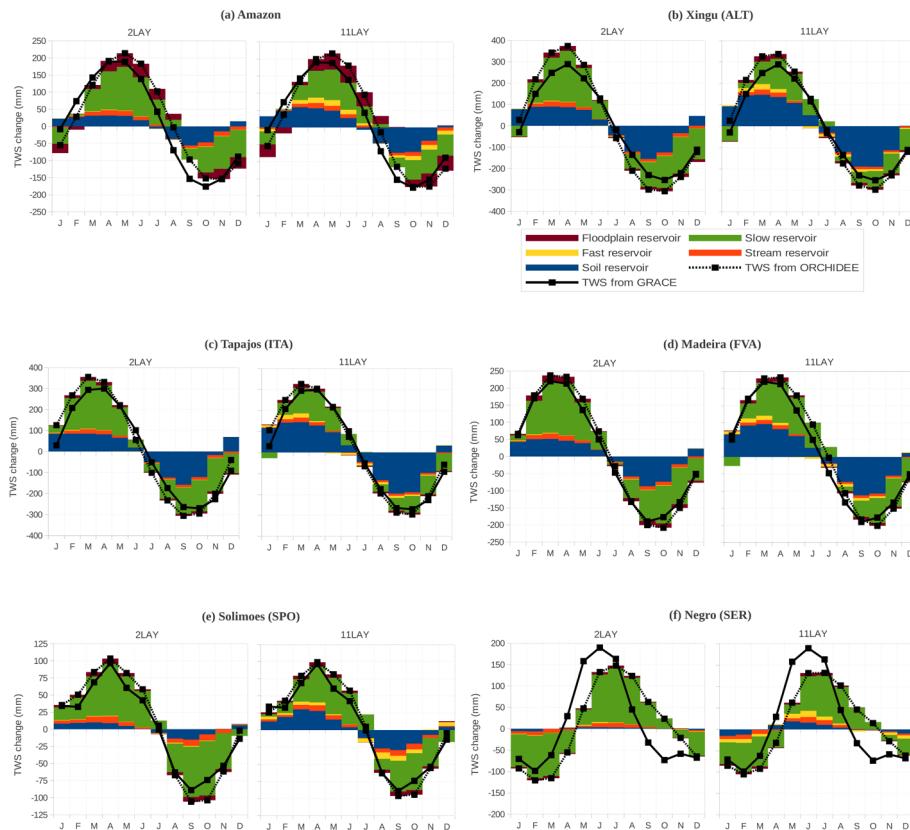


Fig. 3. Monthly mean change of the water storage components (mm) in the different water reservoirs of ORCHIDEE for simulations 2LAY (left) and 11LAY (right), for each sub-basin, averaged over the period 2003–2008. The thick black line represents the independent GRACE observation. The dotted black line is the sum of water storage across all the ORCHIDEE water reservoirs.

Two soil hydrology formulations tested for the Amazon basin

M. Guimberteau et al.

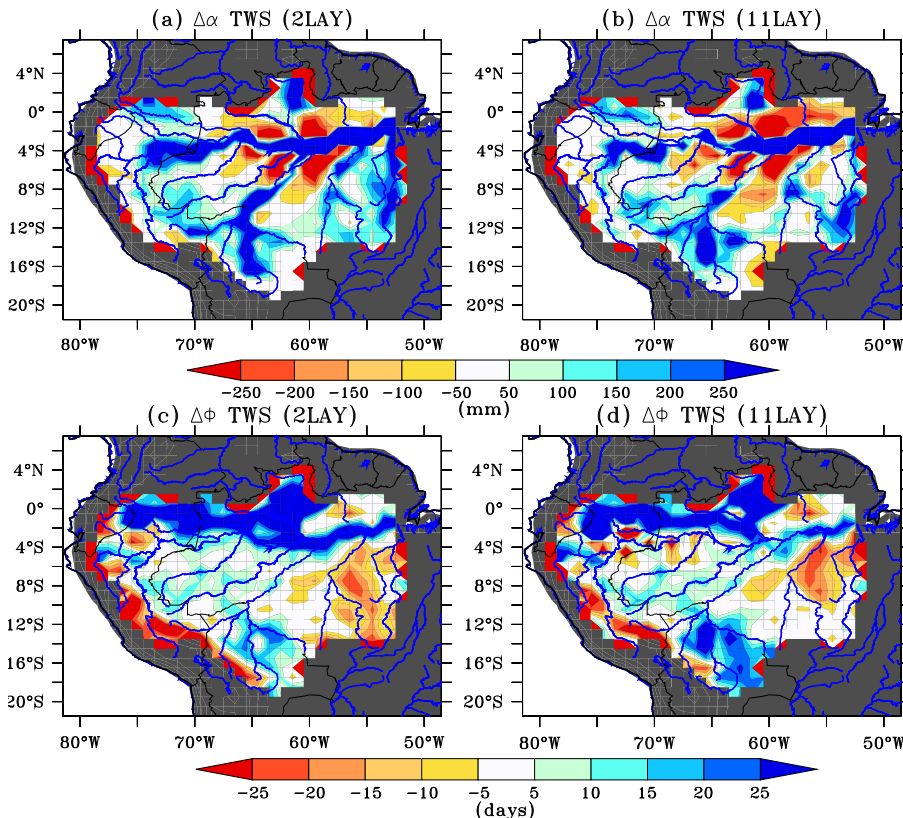


Fig. 4. Differences in **(a, b)** amplitude ($\Delta\alpha$ in mm) and **(c, d)** phase ($\Delta\phi$ in days) of TWS between simulations (2LAY and 11LAY) and GRACE, averaged over the period 2003–2008.



Two soil hydrology formulations tested for the Amazon basin

M. Guimbeteau et al.

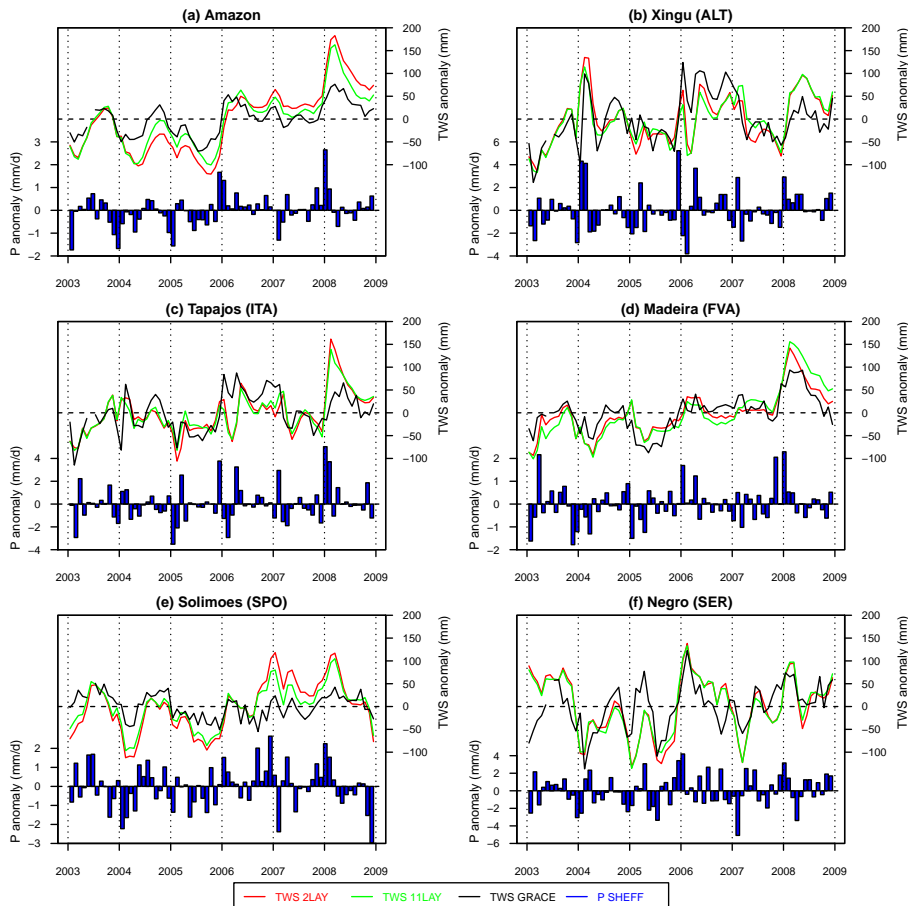


Fig. 5. Interannual monthly variation of deseasonalized TWS (mm) from simulations (2LAY and 11LAY) compared to GRACE data, and Sheffield precipitation anomalies (mm d^{-1}), for each sub-basin, for the period 2003–2008.

Two soil hydrology formulations tested for the Amazon basin

M. Guimberteau et al.

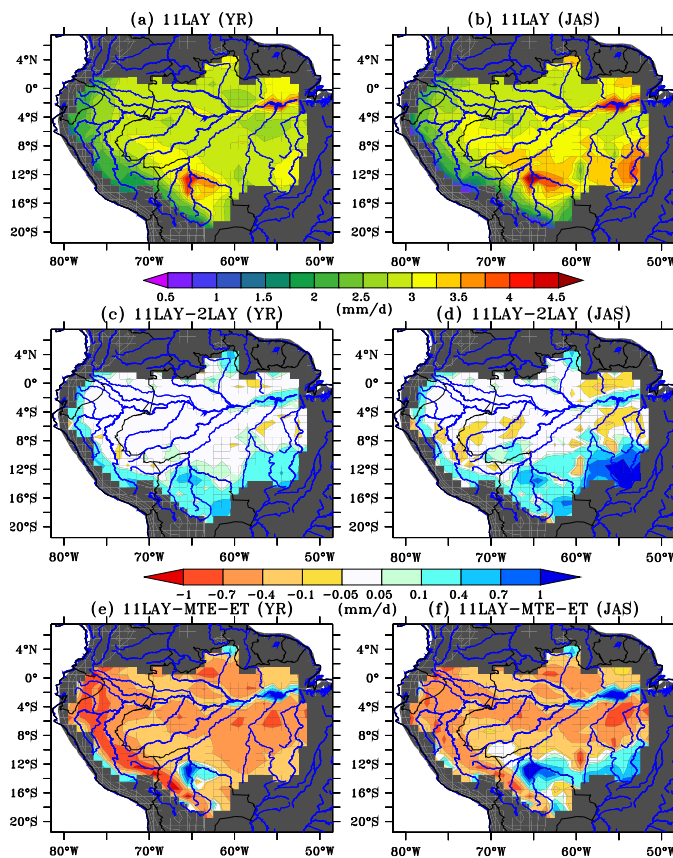


Fig. 6. Mean ET (mm d^{-1}) simulated by 11LAY over the Amazon basin, averaged over (a) the complete year and (b) JAS, averaged over the period 1980–2008. Differences with (c, d) 2LAY and (e, f) MTE-ET.

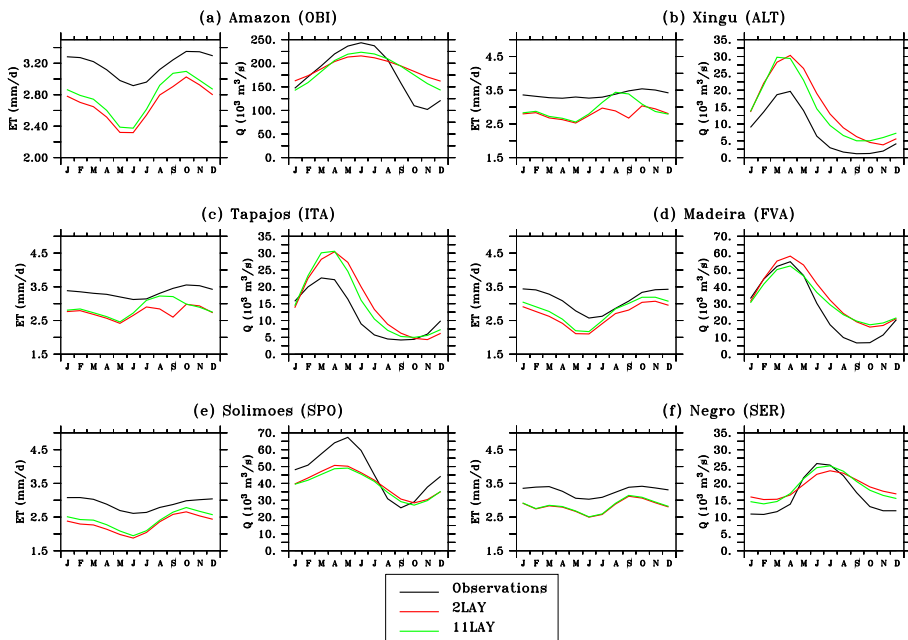


Fig. 7. Monthly mean seasonal ET averaged over the different sub-basins (mm d^{-1}) and river discharge at the gauging stations ($\text{m}^3 \text{s}^{-1}$), from 2LAY and 11LAY simulations compared to the observations, averaged over the period 1980–2008.

Two soil hydrology formulations tested for the Amazon basin

M. Guimberteau et al.

Title Page

Abstract

Introduction

Conclusions

References

Tables

Figures



Back

Close

Full Screen / Esc

[Printer-friendly Version](#)

Interactive Discussion

Two soil hydrology formulations tested for the Amazon basin

M. Guimberteau et al.

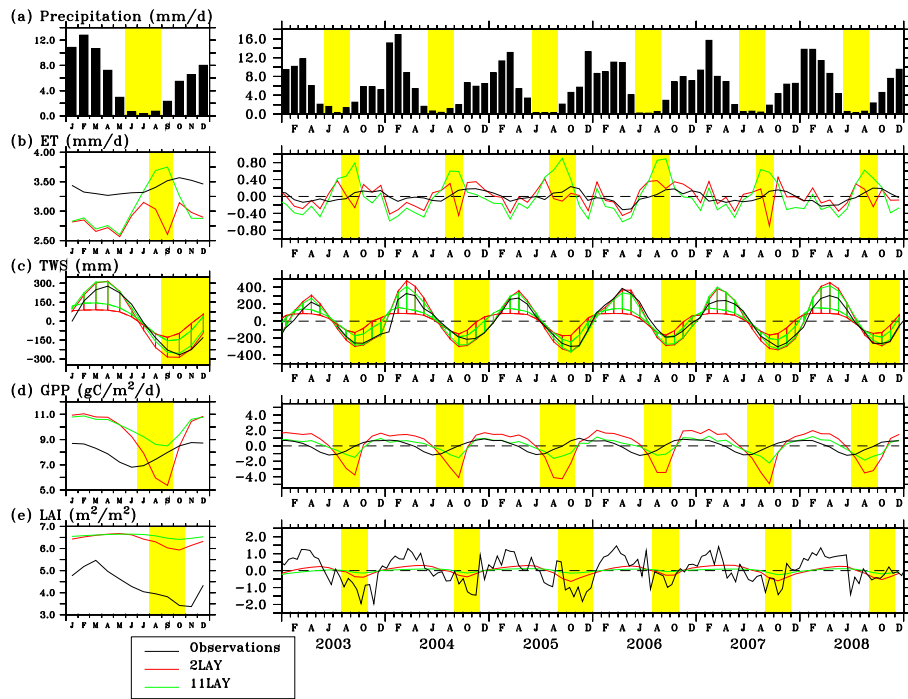


Fig. 8. Seasonal cycle (left panels) and interannual monthly variation of anomaly (except precipitation) (right panels) in (a) precipitation (mm d^{-1}), (b) ET (mm d^{-1}), (c) TWS change (mm) (d) GPP ($\text{g C m}^{-2} \text{d}^{-1}$) and (e) LAI ($\text{m}^2 \text{m}^{-2}$) averaged over the Xingu sub-basin, from simulations (2LAY and 11LAY) and observations, for the period 2003–2008. For anomaly computation, the mean value over the period considered was subtracted from each monthly value of the variable. The yellow band indicates the dry season (in a) and the period during which the difference in results between 2LAY and 11LAY is high (in b to e). The shaded area (red and green in c) corresponds to the simulated anomaly of water stored in reservoirs other than the soil reservoir (dotted red and green lines in c).

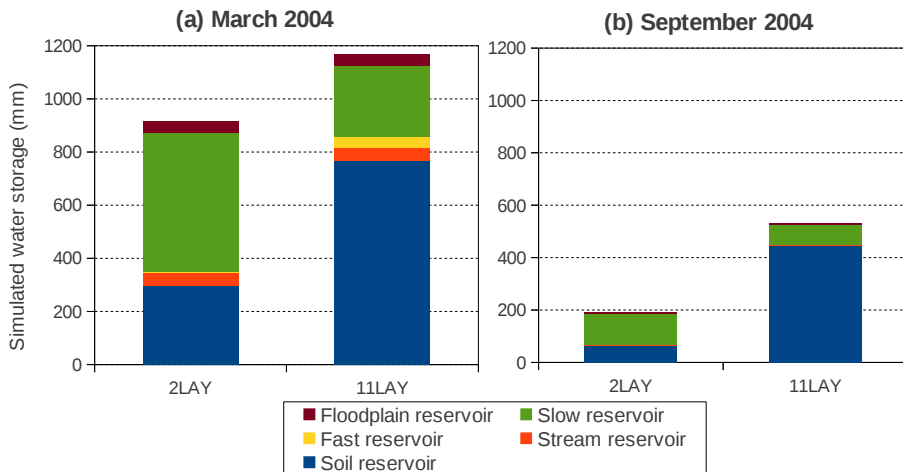


Fig. 9. Monthly water storage distribution in the different reservoirs of ORCHIDEE (mm) between 2LAY and 11LAY, averaged over the Xingu sub-basin, during two contrasting months of 2004: **(a)** March (after the wet season) and **(b)** September (after the dry season).

Two soil hydrology formulations tested for the Amazon basin

M. Guimberteau et al.

Title Page

Abstract

Introduction

Conclusion

References:

Tables

Figures



Two soil hydrology formulations tested for the Amazon basin

M. Guimberteau et al.

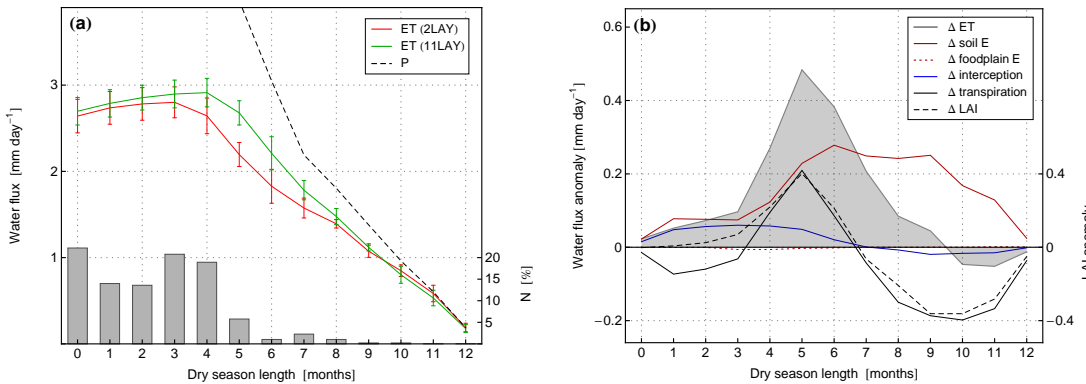


Fig. 10. **(a)** Mean annual ET (mm d^{-1}) from simulations (2LAY and 11LAY) and Sheffield precipitation (mm d^{-1}) over the Amazon basin as function of the dry season length (DSL in months, see Sect. 4.5 for its definition). Solid lines represent the mean ET and spread (1 std) within moving bins of DSL of 1 month, according to the two simulations. The values are obtained from individual grid cells of the simulated domain. Density of grid cells (N in %) associated with each DSL value is given in the histogram. **(b)** Differences of mean annual ET (mm d^{-1}), its components (mm d^{-1}) and LAI ($\text{m}^2 \text{m}^{-2}$) between 11LAY and 2LAY according to the DSL, over the Amazon basin, for the period 1980–2008.

- [Title Page](#)
- [Abstract](#) [Introduction](#)
- [Conclusions](#) [References](#)
- [Tables](#) [Figures](#)
- [◀](#) [▶](#)
- [◀](#) [▶](#)
- [Back](#) [Close](#)
- [Full Screen / Esc](#)
- [Printer-friendly Version](#)
- [Interactive Discussion](#)